Åbo Akademi
University

Functionalisation of spruce *O*-acetyl galactoglucomannans for barrier and composite applications

Victor Kisonen

Laboratory of Wood and Paper Chemistry
Faculty of Science and Engineering
Åbo Akademi University
Åbo, Finland, 2015

Victor Kisonen

Born 1972, Masku, Finland
M.Sc. in Chemistry, 2005
Turku University

Started Ph.D research at the Laboratory
of Wood and Paper Chemistry in 2009
Åbo Akademi University, Finland

Functionalisation of spruce *O*-acetyl-galactoglucomannans for barrier and composite applications

Victor Kisonen

Academic Dissertation

Laboratory of Wood and Paper Chemistry

Johan Gadolin Process Chemistry Centre

Faculty of Science and Engineering

Åbo Akademi University

Åbo, Finland, 2015

Supervisors:

Professor Stefan Willför

Laboratory of Wood and Paper Chemistry

Johan Gadolin Process Chemistry Centre

Åbo Akademi University

Åbo, Finland

Docent Chunlin Xu

Laboratory of Wood and Paper Chemistry

Johan Gadolin Process Chemistry Centre

Åbo Akademi University

Åbo, Finland

Reviewer:

Senior Research Associate, PhD Elisabeth Sjöholm

Innventia Ab

Stocholm, Sweden

Reviewer and Opponent:

Research Professor Ali Harlin

VTT Technical Research Centre of Finland

Esbo, Finland

ISBN 978-952-12-3286-2

Painosalama Oy – Turku, Finland 2015

Abstract

The increasing use of energy, food, and materials by the growing population in the world is leading to the situation where alternative solutions from renewable carbon resources are sought after. The growing use of plastics depends on the raw-oil production while oil refining are politically governed and required for the polymer manufacturing is not sustainable in terms of carbon footprint. The amount of packaging is also increasing. Packaging is not only utilising cardboard and paper, but also plastics. The synthetic petroleum-derived plastics and inner-coatings in food packaging can be substituted with polymeric material from the renewable resources. The trees in Finnish forests constitute a huge resource, which ought to be utilised more effectively than it is today. One underutilised component of the forests is the wood-derived hemicelluloses, although Spruce *O*-acetyl-galactoglucomannans (GGMs) have previously shown high potential for material applications and can be recovered in large scale.

Hemicelluloses are hydrophilic in their native state, which restrains the use of them for food packaging as non-dry item. To cope with this challenge, we intended to make GGMs more hydrophobic or amphiphilic by chemical grafting and consequently with the focus of using them for barrier applications. Methods of esterification with anhydrides and cationic etherification with a trimethyl ammonium moiety were established. A method of controlled synthesis to obtain the desired properties by the means of altering temperature, reaction time, the quantity of the reagent, and even the solvent for purification of the products was developed. Numerous analytical tools, such as NMR, FTIR, SEC-MALLS/RI, MALDI-TOF-MS, RP-HPLC and polyelectrolyte titration were used to evaluate the products from different perspectives and to acquire parallel proofs of their chemical structure.

Modified GGMs with different degree of substitution and the correlating level of hydrophobicity was applied as coatings on cartonboard and on nanofibrillated cellulose-GGM films to exhibit barrier functionality. The water dispersibility in processing was maintained with GGM esters with low DS. The use of chemically functionalised GGM was evaluated for the use as barriers against water, oxygen and grease for the food packaging purposes. The results show undoubtedly that GGM derivatives exhibit high potential to function as a barrier material in food packaging.

Keywords

Norway spruce, *O*-acetyl-galactoglucomannans, hemicelluloses, esterification, cationic etherification, chemical modification, hydrophobicity, NMR, polyelectrolyte titration, grease barrier, packaging, biocomposite, oxygen permeability

Suomenkielinen tiivistelmä

Maailman väkiluvun kasvaessa lisääntyvän energian, ruoan ja materiaalien käyttö johtaa tilanteeseen, jossa tarvitaan vaihtoehtoisia ratkaisuja uusiutuvista luonnonvaroista. Lisääntyvä muovien käyttö on riippuvainen raakaöljyn saatavuudesta ja öljynjalostus on poliittisesti värittynyttä. Öljyä tarvitaan myös polymeerituotantoon, jonka hiilijalanjälki ei ole ekologisesti kestävä. Myös pakkauksien määrä on kasvussa. Pakkauksissa käytetään kartongin ja paperin lisäksi myös öljypohjaisia muoveja. Ruokapakkausten synteettiset öljypohjaiset muovit ja sisäpintojen päällysteet voidaan korvata uusiutuvien luonnonvarojen polymeerisillä materiaaleilla. Suomen metsissä olevat puut ovat resurssi, jota kannattaisi hyödyntää nykyistä tehokkaammin. Puiden hemiselluloosat ovat yksi liian vähän hyödynnetyistä komponenteista, vaikka kuusen galaktoglukomannaaneja voidaan eristää suuressa mittakaavassa ja nämä ovat osoittautuneet arvokkaiksi materiaalisovelluksissa.

Hemiselluloosat ovat luonnostaan hydrofiilisiä. Tämä ominaisuus rajoittaa niiden soveltuvuutta nestepitoisten tuotteiden ruokapakkauksiin. Haastetta lähdettiin ratkaisemaan galaktoglukomannaanien muuttamisella hydrofobiseksi tai amfifiiliseksi kemiallisella oksastuksella. Muunneltuja galaktoglukomannaaneja voidaan siten käyttää pakkausten barrierisovelluksissa. Esteröinnit tehtiin anhydrideillä ja kationiset eetteröinnit tehtiin trimetyyliammoniumkloridilla. Haluttu substituutioaste tai reaktiotehokkuus saavutettiin menetelmillä, joissa muutettiin reaktiolämpötilaa ja -aikaa, reagenssien määrää ja jopa liuotinta puhdistusta varten. Useiden analyyttisten menetelmien, kuten NMR, FTIR, SEC-MALLS/RI, MALDI-TOF-MS, RP-HPLC ja polyelektrolyyttititraus, avulla arvioitiin reaktiotuotteita erilaisista näkökulmista ja saatiin rinnakkaisia todisteita kemiallisista rakenteista.

Muunneltuja galaktoglukomannaaneja, joilla on erilainen substituutioaste ja sitä korreloiva hydrofobisuus, käytettiin päällysteinä kartongilla ja nanofibrilliselluloosa-galactoglukomannaani -kalvoilla barrieriominaisuuksien saavuttamiseksi. Alhaisen substituutioasteen GGM oli veteen dispergoituvaa ja soveltui siten prosessoitavaksi. Muokattujen galaktoglukomannaanien käyttöä arvioitiin veden, hapen ja rasvan estäjänä ruokapakkauksia varten. Tulokset näyttävät selvästi, että galaktoglukomannaanien johdannaisilla on korkea potentiaali toimia barriereina ruokapakkauksissa.

Svensk sammanfattning

Den ökande folkmängden i världen använder mera energi, mat och material, vilket leder till en situation där alternativ från förnybara naturresurser behövs. Den växande användningen av plaster är beroende av våra råoljereserver. Oljeraffinering, som är politiskt styrd och nödvändig för polymertillverkningen, är inte hållbar vad gäller kolspåret. Behovet av förpackningsmaterial ökar också ständigt och här används oljebaserade plaster, förutom kartong och papper. Syntetiska oljebaserade plaster och inre skikt i livsmedelsförpackningar kan ersättas med polymera material från förnybara resurser. Våra finska skogar utgör en enorm resurs som borde utnyttjas bättre än idag. Vedbaserade hemicellulosor är en underutnyttjad råvara även om granens acetylgalaktoglukomannaner tidigare har visat stor potential i olika materialapplikationer och även kan utvinnas i stor skala.

Naturliga hemicellulosor är hydrofila, vilket begränsar deras användning i livsmedelsförpackningar för fuktiga livsmedel. För att övervinna denna utmaning var vårt mål att göra galaktoglukomannanerna mera hydrofoba eller amfifila genom kemisk modifiering för att sen kunna använda dem som barriärer i olika applikationer. Vi utvecklade därför metoder för förestring med anhydrider och katjonisk företring med trimetylammoniumgrupper. Vi etablerade metoder för kontrollerad syntes för att uppnå önskad substitutionsgrad eller reaktivitet genom att variera temperatur, reaktionstid, mängd reagens och lösningsmedel för rening av produkterna. Ett flertal analytiska metoder, såsom NMR, FTIR, SEC-MALLS/RI, MALDI-TOF-MS, RP-HPLC och polyelektrolyt-titrering, användes för att karakterisera produkterna och bekräfta deras kemiska struktur.

De modifierade galaktoglukomannanderivaten med olika substitutions- och hydrofobicitetgrad utnyttjades för att bestryka kartong eller filmer av nanocellulosa och galaktoglukomannaner för att ge barriäregenskaper. Galaktoglukomannanestrarna med låg substitutionsgrad gick att dispergera i vatten och kunde med fördel användas i bestrykning. De kemiskt modifierade galaktoglukomannanernas barriäregenskaper mot vatten, syre och fett utvärderades med tanke på deras användning i livsmedelsförpackningar. Resultaten visar klart att galaktoglukomannanderivaten visar hög potential att kunna användas i dylika produkter.

List of the original publications

I. Kisonen, V., Xu, C., Eklund, P., Lindqvist, H., Sundberg, A., Pranovich, A., Sinkkonen, J., Vilaplana, F., and Willför, S. (2014). Cationised *O*-acetyl galactoglucomannans: synthesis and characterisation. Carbohydr. Polym. *99*, 755–764.

II. Kisonen, V., Eklund, P., Auer, M., Sjöholm, R., Pranovich, A., Hemming, J., Sundberg, A., Aseyev, V., and Willför, S. (2012). Hydrophobication and characterisation of *O*-acetyl-galactoglucomannan for papermaking and barrier applications. Carbohydr. Res. *352*, 151–158.

III. Kisonen, V., Xu, C., Bollström, R., Hartman, J., Rautkoski, H., Nurmi, M., Hemming, J., Eklund, P., and Willför, S. (2014). *O*-acetyl galactoglucomannan esters for barrier coatings. Cellulose *21*, 4497–4509.

IV. Kisonen, V., Prakobna, K., Xu, C., Salminen, A., Mikkonen, K.S., Valtakari, D., Eklund, P., Seppalä, J., Tenkanen, M., and Willför, S. (2015). Composite films of nanofibrillated cellulose and *O*-acetyl galactoglucomannan (GGM) coated with succinic esters of GGM showing potential as barrier material in food packaging. J. Mater. Sci. *50*, 3189–3199.

Contribution of the author

The author of the theses is the main author in all four publications (I-IV). The author designed and carried out the experimental work with the exception of the experimental work of the NFC-GGM film preparation, the dynamic mechanical analysis and oxygen permeability analysis in the paper IV. SEC-MALLS, WVTR, grease barrier and contact angle analysis which was implemented with the collaboration of the co-authors. Help of specialist was obtained for the experimental work with SEM in papers III-IV and thermal analysis in papers I-II and MALDI-TOF-MS with papers I and III.

Supporting publications

Prakobna, K., Kisonen, V., Xu, C., and Berglund, L.A. (2015). Strong reinforcing effects from galactoglucomannan hemicellulose on mechanical behavior of wet cellulose nanofiber gels. J. Mater. Sci. *50*, 7413–7423.

Mänttari, M., Manasrah, M. Al, Strand, E., Laasonen, H., Preis, S., Puro, L., Xu, C., Kisonen, V., Korpinen, R., and Kallioinen, M. (2015). Improvement of ultrafiltration performance by oxidation treatment in the recovery of galactoglucomannan from wood autohydrolyzate. Sep. Purif. Technol. *149*, 428–436.

Kisonen, V., Xu, C., Prakobna, K. and Willför, S. (2014). Barrier films of nanofibrillated cellulose and *O*-acetyl galactoglucomannan (GGM) coated with succinic esters of GGM. International Conference on Bio-based Materials and Composites (ICBMC'14), - Montreal- Canada, Proceedings pp. 156, ID-123, (Poster precentation).

Kisonen, V., Eklund, P., Xu, C., Nurmi, M., Bollström, R., Hartman, J., Rautkoski, H. and Willför, S. (2013). *O*-acetyl- galactoglucomannans esters for barrier applications. Composites week @ Leuven and TexComp-11: 16-20 September (Oral presentation).

Kisonen, V., Eklund, P., Auer, M., Sjöholm, R., Pranovich, A., Hemming, J., Sundberg, A., Aseyev, V. and Willför, S. (2011). Modification and characterisation of *O*-acetyl galactoglucomannans. Italic 6 - Science & Technology of Biomass: Advances and Challenge Proceedings pp. 42-45 (Poster precentation).

List of relevant abbreviations

amm	[*O*-(2-hydroxy-3-methylammonium)propyl]+
AX	arabinoxylan
CA	contact angle
Cat-GGM	cationic ether of GGM
Cat-GGM-Ac	acetylated cationic ether of GGM
CHMAC	3-chloro-2-hydroxypropyltrimethylammonium chloride
CMC	carboxymethyl cellulose
CM-MFC	carboxymethyl microfibrillated cellulose
DEPT-135	Distortionless Enhancement by Polarization Transfer with 135^o angle
DMA	dynamic mechanical analysis
DMAP	dimethylaminopyridine
DS	degree of substitution
EA	elemental analysis
ETA	2,3-epoxypropyltrimethylammonium chloride
Eqv.	equivalents
GGM	spruce *O*-acetyl-galactoglucomannan, also high-molar-mass spruce *O*-acetyl-galactoglucomannan (III)
GGM-Bz	benzoyl ester of GGM
GGM-Bu	butyric ester of GGM
GGM-Ph	phthalic ester of GGM
GGM-Su	succinic ester of GGM
HMBC	Heteronuclear Multiple-Bond Correlation Spectroscopy
LMW-GGM	low-molar-mass *O*-acetyl-galactoglucomannan
NFC	nanofibrillated cellulose

List of relevant abbreviations

M_w	weight-average molar mass
NMR	nuclear magnetic resonance spectroscopy
MALDI-TOF-MS	matrix-assisted laser desorption/ionisation time-of-flight mass spectrometer
OPU	O-(2-oxo)propyl unit
OP	oxygen permeability
OTR	oxygen transmission rate
PEI	cationic polyethyleneimine
PT	polyelectrolyte titration
PET	polyethylene terephthalete
PHA	polyhydroxyalkanoate
PLA	polylactic acid
RE	reaction efficiency
R.H.	relative humidity
RP-HPLC	Reverse phase high performance liquid chromatography
SEC-MALLS	size exclusion chromatography with multi-angle laser-light-scattering detector
SEM	scanning electron microscopy
SU	sugar unit
TGA	thermal gravimetric analysis
T_d	decomposition temperature
T_g	glass transition temperature
WVTR	water vapour transmission

Contents

1. Introduction

The rapidly increasing population in world has a growing need of food, energy and materials. This challenge can be approached by the more efficient and sustainable use of natural resources and by decreasing dependence on fossil oils. It is a major issue to develop novel and renewable materials out of wood or by utilising existing process streams that today go to waste or incineration. Agricultural waste and wood offer easily accessible natural fibres for composite material applications (Jana and Prieto, 2002; Thamae and Bailie, 2008). The increasing use of energy with correlating carbon dioxide emissions and the shortage of clean water and food further emphasise the point to explore new sustainable alternatives to replace the oil-based materials. Moreover, the legislative framework in the European Union implements the accessibility of biomaterials to the market. The drastic growth of the bioplastic market can boost the further evolution of the bio-economy in Europe (Institute of Bioplastics and Biocomposites, 2013).

Forests have provided the economic well-being in Finland for centuries. At first it was the production of tar, and from the nineteenth century paper production began. Paper production in Europe and America has been decreasing lately, which encourages companies to search for new solutions. Nowadays wood as raw materials provides opportunities to be used for totally new means, i.e. for materials and pharmaceutical and smart packaging applications. Trees produce biopolymers and extractives. Biopolymers from trees in native state are mainly hemicelluloses, cellulose and lignin. These can be isolated from the wood matrix by extraction. Hemicelluloses can be isolated also from side streams in pulp and paper mills. *O*-acetyl-galactoglucomannan (GGM) is the major hemicellulose in Norway spruce (*Picea abies,* family *Pinaceae*). Norway spruce is the major tree species in Finland along with another conifers, Scot pine (*Pinus sylvestris*). GGM possesses high potential in industrial applications, for instance as incorporated into composite materials or as rheology modifier in paints and in food (Mikkonen and Tenkanen, 2012; Xu et al., 2009a). Moreover, hemicelluloses can be turned into platform chemicals, such as ethanol, furfural and acetic acid (Bhaumik et al., 2014; Caratzoulas et al., 2014; Cunha and Gandini, 2010; Deuss et al., 2014; Heinze et al., 2006).

Regardless of the high potential for chemicals and applications, hemicelluloses are present in papermaking as ineffectively utilised biopolymers. There is a chicken-and-egg causality dilemma with hemicelluloses as a raw material for industrial applications. In order to produce hemicelluloses with moderate cost at a large production capacity, there ought to be a demand and a commercial use for such biopolymers. However, successful commercial applications would not be established unless there exist large-scale production facilities. On the other hand, no large scale production would appear either, unless there was certainty of an end use for the raw material. On the positive side, there are now motives to break up this vicious cycle. For instance, recently there has been research on pilot-scale production facilities of wood-derived hemicelluloses (Manasrah et al., 2012; Thomsen et al., 2008; Willför et al., 2003b). A modern biorefinery plant based on wood material is able to produce cellulose, hemicelluloses, lignin, extractives and energy in an economical manner. In this study we utilised enriched GGM hemicelluloses from a mechanical pulp mill and from hot water extraction of spruce stemwood.

Petroleum-based plastics contribute to global warming. A part of the plastics is ending up in landfills, energy production, and recycling for further use. However, the non-biodegradable plastic waste depositions on land and in oceans are a worldwide challenge and a hurdle. Plastics such as polystyrene, break up to micro-sized particles and find their way into living organisms, like animals and plants (Jayasiri et al., 2013; Nyström, 2014). Bioplastics originate from renewable biological origin and can be biodegradable at the end of their life cycle (Shah et al., 2008). As biodegradable material is eventually discarded, it can be composted, and the life cycle may continue. "Biodegradable" and "compostable" are frequently confused (Shah et al., 2008). “Compostable" indicates that the process will result in compost or humus. The alternatives to conventional plastics may be biodegradable starch, cellulose, and hemicellulose derivatives. However, the use of starch for materials and energy is increasing its price as a food ingredient too, while the use of GGM does not compete with the food chain.

Natural resources are inexpensive and readily available. The use of natural fibres instead of oil-based polymers and glass fibres as reinforcing agents in material applications reduces the environmental impact to a great deal. This can be contemplated from the perspective of the developing countries; insufficient education, shortage of investing capital and corruption make them to be dependent of the imported energy and refined products (Ekouevi and Adepoju, 1995). There is aspiration though; the case study has demonstrated that the resources of the developed and developing countries can be potentially harnessed by the means of implementing the technology for instance to produce natural fibre composites from local resources (Thamae and Bailie, 2008). Flexural properties of composites from waste material can thus be optimised with regards to cost and local availability of materials. Consequently, there are ethical and economical motives to produce 100% bio-based material to replace conventional non-biodegradable petrolium-derived plastics, e.g. in packaging and in consumer goods. Plant-derived polysaccharides with added functionality may have a substantial role in this scenario. Hence we studied GGM-based derivatives for coating and composite applications.

Hemicelluloses may have relatively low molar mass, but incorporated with other polymers in composites for property enhancer, they can be suitable for packaging. In this study, the chemical and physical structure-barrier property relationships of modified GGMs were evaluated as coatings or composites. In short, this study seeks approaches for using chemically modified spruce GGM for layering novel cellulose-based packaging materials to replace conventional petroleum-based polymers (Figure 1).

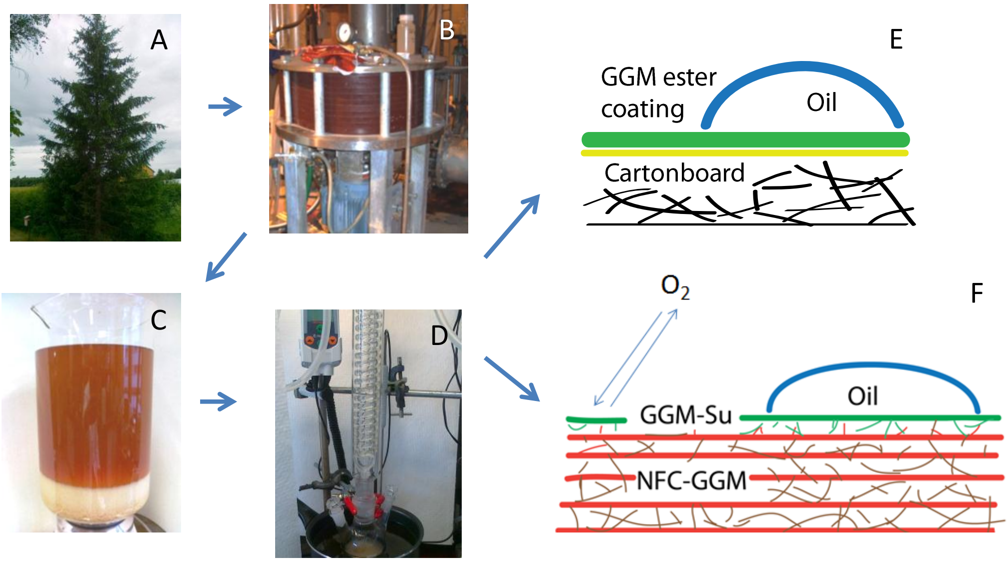

Figure 1. Illustration of the approach of this study. Norway spruce (A) GGM was recovered from process waters in thermomechanical pulp mills by ultrafiltration (B). GGM was purified by washing with ethanol-water (C). GGM was modified by derivatisation of GGM (D) followed by barrier-application as GGM ester coatings on cartonboard or as a coating on NFC films (E) and as a filler in NFC network (F).

2. Hypothesis and objectives of this study

The environmental concerns towards petroleum-based materials and coatings favour the use of sustainable resources of raw materials, like hemicelluloses and their derivatives. The challenge for the use of hemicelluloses for material applications is their sensitivity towards water and their low molar mass compared to synthetic polymers. This challenge we wanted to overcome for spruce GGM. The hypothesis of the study is that chemically functionalised GGM can be used as barriers in food packaging applications in biocomposites for various uses.

The main objectives of work were:

-to render GGM hydrophobic by chemical grafting

-to evaluate the water, oxygen, and grease barrier properties of the barrier coatings of the obtained GGM derivatives

-to evaluate the behaviour of the GGM derivatives with nanofibrillated cellulose as reinforcing network in composites

-to use a range of analytical tools to determine the chemical structures of the GGM derivatives

-to synthesise cationised GGM and acetylated cationised GGM to meet the demands of polyelectrolyte layering in composites

3. Background

3.1. Polysaccharides and hemicelluloses

A growing desire is to discover new macromolecular raw materials from renewable resources (Cunha and Gandini, 2010). The major group of macromolecules are polysaccharides, which are carbohydrates formed by the connection of monosaccharide units through hemiacetal or hemiketal linkages as five and six carbon sugars, which form pentose and hexose rings, respectively. There is a large variety of naturally occurring polysaccharides, which originate from plants, micro-organisms, fungi, marine organism, and even animals (Ramesh and Tharanathan, 2003). Monosaccharide units also exist as short oligomeric or polymeric repeating units linked to other biopolymers, as e.g. in glycoproteins and glycolipids. These unique biomolecules can be responsible for structural performance, energy storage, and information connections (Ramesh and Tharanathan, 2003).

In this study, we use the term *hemicelluloses* for the non-cellulosic and non-starch hetero-polysaccharides, which are present in wood and plant cell tissue. The botanical source, the type of plant tissue, as well as the isolation, extraction, and purification methods of hemicelluloses make a distinct impact on the chemical and physical appearance of isolated hemicelluloses and on the sugar unit ratios (Hansen and Plackett, 2008; Um and van Walsum, 2010; Willför et al., 2008). Hemicelluloses are biosynthesised in large measures in the majority of trees and herbaceous plants. They are heterogeneous and branched chemical structures of sugar monomer units. They possess an amorphous morphology and are usually in close connection with cellulose in their native state (Gatenholm and Tenkanen, 2004; Hansen and Plackett, 2008). Hemicelluloses are often bonded to cell-wall constituents, also other than cellulose, such as proteins, lignin, and phenolic compounds by covalent and hydrogen bonds, and also by ionic and hydrophobic interactions (Peng et al., 2012).

GGMs are the main hemicelluloses in softwoods. GGM is a heteropolysaccharide and has a structure of (1→4)-linked β-D-mannopyranosyl and (1→4)-linked β-D-glucopyranosyl units in the main chain, while (1→6)-linked α-galactopyranosyl units are attached to mannose units only. *O*-acetyl groups are attached to C2 and C3 positions of the mannose units in the main chain. It is suggested, that the order of the sugar units are mostly but not entirely random (Jones et al., 1957; Timell and Syracuse, 1967). However, the current consensus seems to agree that sugar residues and acetyl groups are random in GGM (Hannuksela and Hervé du Penhoat, 2004; Willför et al., 2003b). Norway spruce GGM can be recovered from process waters in thermomechanical pulp mills by ultrafiltration. This GGM has an average molar ratio 2.3:1:0.6 of mannose, glucose, and galactose, respectively (Xu et al., 2009b). Polymeric GGM can also alternatively be isolated from wood by hot-water extraction (Song et al., 2008; Grenman et al., 2011; Krogell et al., 2013; Rissanen et al., 2014; Von Schoultz, 2014).

3.2. Chemical modification of polysaccharides

3.2.1. Overview

Hydrophilic biopolymers may be altered hydrophobic by appropriate modifications either by physical treatment or chemical reactions applied to the surface or the entity of the concerned polysaccharide (Cunha and Gandini, 2010). Further, chemical modification processes of biomass have been developed as a parallel method to thermochemical and enzymatic ways of conversion (Chatterjee et al., 2014). In this study, we focus on the chemical treatments. Homogeneous chemical processes with hemicelluloses provide much higher modification yield than heterogeneous processes (Durand and Dellacherie, 2006). The distribution of hydrophobic substituents along the polymer backbone can be blocked in a heterogeneous reaction medium, where the substrate is not dissolved (Hirrien et al., 1997). The usual way to modify the polysaccharides takes place in liquid phase resulting in covalent bonds.

3.2.2. Etherification of polysaccharides with an ionic moiety

Etherification with a group of ammonium moiety is often carried out with 3-chloro-2-hydroxypropyltrimethylammonium chloride (CHMAC), where the chloride ion acts as leaving group (Ebringerova et al., 1994) (Figure 2) or by group opening with 2,3-epoxypropyltrimethylammonium chloride (ETA) (Bigand et al., 2011). Cationic groups in polysaccharides often consist of trimethylammonium chloride or one of the methyl groups is replaced with an aliphatic chain (Wei et al., 2008). The DS value 1.5 for starch was achieved by carrying out the cationisation reaction two times (Heinze et al., 2004). The ETA reagent and hemicellulose concentrations were optimised for xylan and galactomannan-type hemicellulose cationisation. High concentration of xylan yielded good mass balances with moderate ETA concentrations (Bigand et al., 2011). Alkalisation in water increased the reactivity also with insoluble xylans (Ebringerova et al., 1994). Cationisation of polysaccharides can be carried out in heterogeneous manner in ethanol/water or in homogenous manner in DMSO (Heinze et al., 2004; Ren et al., 2007). Homogenous systems yielded higher DS due to better access of reagent to the dissolved hemicellulose (Ren et al., 2007, 2008).

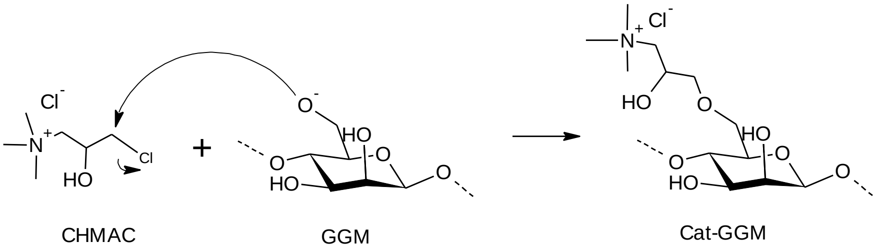

Figure 2. Cationic etherification of GGM with 3-chloro-2-hydroxypropyltrimethylammonium chloride (CHMAC) in the presence of sodium hydroxide.

Cationic etherification has also been carried out with trimethylglycine (betaine amino acid) (Auzély-Velty, 2011). Diverging from a synthesis in a solvent, a reactive extrusion approach was applied in starch cationisation (Moad, 2010). The reactive extrusion has advantages of high conversion efficiency, an ability to remove or recycle excess reagents and by-products, and an efficient rate of production.

Nuclear magnetic resonance spectroscopy (NMR) is the common method to solve the structure of ionic hemicellulose derivatives (Bigand et al., 2011; Dax et al., 2014). Also polyelectrolyte titration is a common method to determine charge density of e.g. cationic starch regarding papermaking process. Polyelectrolyte titration with a particle charge detector can for instance be used to determine anionic charge in humic substances (Tan et al., 2011).

3.2.3. Chemical hydrophobisation of polysaccharides

Chemical modification of polysaccharides must as rule of thumb involve reagent, usually solvent, and catalyst for the synthesis and the appropriate purification method of the product. The purification is meant to dismiss possible non-relevant non-polymeric and polymeric compounds. The synthesis may include protecting groups or the substitution pattern may be implemented with a catalyst, which in particular favours regional substitution (Heinze et al., 2006).

Esterification and etherification often results in a hydrophobic product. Acyl chlorides are common reagents for polysaccharide esterification in homogenous conditions. For instance, starch was benzoylated with benzoyl chloride in pure water at 4 ˚C (Stojanovic et al., 2002). Etherification can be performed with organo chlorides. wheat straw hemicelluloses were benzylated in ethanol-water with benzyl chloride (Ren et al., 2012). A Common system is to use anhydrides, which are rather benign reagents. Over starch was also benzoylated with benzoic anhydride and pyridine, obtaining a maximum DS of 2.0 (Ciusa and Adamo, 1951). Organic solvent was not needed in acetylation using DMAP or methanesulfonic acid as a catalyst in a reaction of xylan with acetic anhydride (Belmokaddem et al., 2011).

GGM acetyl esters can be produced by acetic anhydride and pyridine, having a DS up to 2.7 with an acid pre-treatment of GGM (Xu et al., 2010). As an engrossing detail, acetyl groups seem to be able to migrate from position C2 of native GGM to positions C3 and even C6 during the acetylation. However, (Ekholm et al., 2012) approached the topic by synthesising GGM-mimicking tetrasaccharide units; no acetyl migration was observed in this case. Dextran was esterified to butyric esters to extremely high DS 3.0 with butyric anhydride and dimethylaminopyridine (DMAP) in DMSO (Beesh et al., 2010). Acetylation with vinyl acetate salt and disodium hydrogen phosphate in DMSO favours C2 regioselectivity on starch in comparison to acetic anhydride as reagent (Dicke, 2004). The LiCl/DMF solvent system has been used for dextran, glucan, and xylan esterifications (Heinze et al., 2006), while a LiCl/DMF solvent system with DMAP was successfully used for esterification of hemicelluloses and guar gum with succinic anhydride (Fujioka et al., 2009; Sun et al., 2001). Hence, we decided to use DMAP with LiCl and DMF in this study (I-II).

Arabinoxylans reacted with gaseous trifluoroacetic anhydride to yield a fluorinated product with increased hydrophobic character, exhibiting water contact angle (CA) of 70° (Gröndahl et al., 2006). However, it was not clear, whether surface or bulk modification took place. 18-crown ether and potassium hydroxide catalysed a heated reaction on xylan with benzyl bromide in anhydrous DMSO, rendering perbenzyl ether as a product (Vincendon, 1998). Aprotic acetonitrile was replaced by DMSO and the complete substitution was obtained in one step reaction. The solvent is usually essential in a synthesis, but a solvent-free method has also been used in transesterification: methyl laurate and base-pretreated starch were synthesised to starch laurate at 130 °C (Geng et al., 2010). GGM is hydrophilic but can be altered more hydrophobic e.g. by cross-linking chemically or enzymatically (Mikkonen et al., 2013; Oinonen et al., 2013). Amphiphilic GGM derivatives have been made using fatty acids, or hydrophobic tails of polydimethylsiloxane (Dax et al., 2013a; Lozhechnikova et al., 2014).

3.3. Polysaccharide-based biopolymers and their applications

3.3.1. Overview

It is an immense industrial interest to develop novel and renewable materials out of wood or utilising existing process streams that today go to waste or incineration. The cellulose acetates have acted as the first plastics about 150 years ago (Cunha and Gandini, 2010). They are now considered as bioplastics. Biopolymers bring the advantages of biodegradability and the use of renewable resources. However, the properties like plasticity, mechanical and chemical resistance, hydrophobicity, and the price of the raw-material and its processing have not usually been appropriate enough to replace the synthetic polymers. The main challenge for low cost would be the development of new processes of fabrication. The European Bioplastics Association gives guidelines that the biopolymers made of renewable resources ought to be biodegradable and compostable (Institute of European Bioplastics and Biocomposites, 2013). Plastics based on renewable resources do not necessarily have to be biodegradable or compostable. On the other hand, biodegradable materials do not necessarily need to be based on renewable materials. The type of chemical structure explicates which microbes are able to biodegrade the material, i.e. synthetic polymers can also be biodegradable and compostable. The bioplastics-based on natural monomers can lose their biodegradability property through chemical modification like polymerization (Siracusa et al., 2008).

Synthetic polymers are usually hydrophobic and hemicelluloses are hydrophilic, which causes inadequate affinity between them. Thus by hydrophobisation of hemicelluloses we increase the level of hemicellulose derivatives being compatible with synthetic polymers (Gatenholm and Tenkanen, 2004). The introduced functionalities on hemicelluloses can be for instance hydrophobicity, polyelectrolyte function, light-emitting property, reinforcing ability with composites, viscosity modifier function, or an enhanced ability for hydrogen bonding. Chemical modification of the structure can lead e.g. to altered molar mass, increased grafting, cross-linking with other polymers, or to changed degree of crystallinity.

Hemicelluloses can be hydrolysed into monomers, which can then be further converted into fine chemicals (Chatterjee et al., 2014). Nevertheless, the polymeric applications for hemicelluloses are so far very limited, because of their low molar mass and varying chemical composition (Salam et al., 2011). Controversially, it can be argued that because of the functional diversities of hemicelluloses and their derivatives, they can be exploited in packaging, coatings, selective separation degradable films, emulsion stabilizers, dietary fibres, nutrition for probiotic bacteria, other nutritional supplements, hydrogels for controlled drug release, drug encapsulation, biosensors in smart and responsive materials, therapeutic applications like wound bandages, printing applications on films and paper and possibly as polyelectrolyte (multi)layering. (Edlund and Albertsson, 2008; Heinze et al., 2006; Leppänen et al., 2013; Liu et al., 2015; Mielonen et al., 2015; Mikkonen et al., 2009; Pahimanolis et al., 2013; Polari et al., 2012; Schoeler et al., 2006; Voepel et al., 2009).

3.3.2. Applications of polysaccharides with an ionic moiety

There have been numerous efforts for utilising cationic polysaccharides and their derivatives. Cationised polysaccharides can be used as flocculants in kaolin suspensions (Bratskaya et al., 2005; Sableviciene et al., 2005; Tian et al., 2010; Wei et al., 2008) or they can be used as an alternative to polyacrylamide-based flocculants in waste water treatment and in papermaking (Kuutti et al., 2011). Physical properties of paper hand-sheets were improved significantly by adding cationised and carboxymethylated hemicelluloses together, while using either of these alone, properties were improved less. Hemicelluloses may be used as a source for the production of wet-end additives in papermaking as a sustainable way of using the agricultural and forestry residues (Ren et al., 2009).

Cationised, carboxymethylated, and iminated GGMs were tested in papermaking properties and they demonstrated deviated behaviour from native GGM (Lindqvist et al., 2013). The cationic GGM ether increased the retention of both fibrous fine material and fillers without deterioration of the mechanical properties, indicating that cationised GGM interacted through an electrostatic mechanism. Iminated GGMs were suggested to act through the alkane chain attached to the reducing end, which oriented towards hydrophobic particles. Carboxymethylated GGMs increased the retention of fibrous materials slightly and was thought to bind with metal ions originating from wood.

Adsorption of cationic polysaccharides and neutral polymers onto solid polymer surfaces has been suggested to mimic the effect of hair conditioner on hair (Guzman et al., 2011). Cationic starch with adjusted charge density is used to adsorb water from rock surface pores in oil reservoirs (Leslie et al., 2005). Cationised konjac glucomannans showed inhibitory effects against some bacterial and fungal species (Yu et al., 2007). Chito-oligosaccharides with quaternary ammonium groups had antibacterial activity against the dental caries *Streptococcus mutans* (Kim et al., 2003). Anionic and cationic starches have been used as interactive polyelectrolyte multi-layers on SiO_2 surfaces (Lundström-Hämälä et al., 2010). Cationic chitosan can also be involved in multi-component coatings for emulsion-based systems to delay the delivery of bioactive lipophilic components used for nutraceuticals or pharmaceuticals (Li et al., 2010).

The mechanism of inkjet ink spreading and absorption on a coated paper with a polyelectrolyte multi-layering system was studied (Mielonen et al., 2015). It was suggested that the outermost polyelectrolyte layer had a major effect on the ink-substrate interaction. The cationic-anionic multi-layer surface treatment influenced the print density, mottling, and ink line performance. The cationic-anionic multi-layer has a strong influence on the adhesion of the colour. Chemical and enzymatic ways were combined in a study, where anionic polysaccharides, such as GGM and *K*-carrageenan, acted as templates for enzymatic polymerisation of conducting polyaniline (Leppänen et al., 2013). This resulted in conducting biocomposites, which can be incorporated into flexible films or coated onto cellulose surfaces.

3.3.3. The synergy of hemicelluloses and cellulose

Due to structural similarity, adhesion between cellulose and certain hemicelluloses leads to excellent affinity and this attribute can be exploited for tailoring functional materials. For instance, xyloglucan was used as a molecular anchor for setting up of polymers to cellulose surfaces (Zhou et al., 2005).

Xyloglucan oligosaccharides were incorporated into xyloglucan by enzymatic means to produce initiator-modified xyloglucan (XG-INI). Adsorption of XG-INI and subsequent atom transfer radical polymerization was utilised to alter the cellulose surface properties and fabricate novel biocomposites. Furthermore, initiator introduction by adsorption did not harm the individual fibres or fibre structures. The reinforcing cellulose fibrils are embedded with cross-linked networks of hemicelluloses and lignin in the wood cell wall. To mimic the plant cell wall structure, composite films of NFC and GGM were prepared and an improved interaction between them was observed (Stevanic et al., 2014). Thus, the composite films of NFC and GGM were used as substrates in this study (IV).

3.3.4. Packaging and barriers

The packaging industry has become the third largest industry in the world and it represents about 2% of the Gross National Product (GNP) in developed countries. Hence it is worthwhile to search for tailored approaches for packaging. In food packaging various properties are required and, for instance, mechanical and optical properties, gas permeability and barrier properties, convenience in use, biodegradability, and the original raw-material can all be tailored to meet the required demands. Multiple layers in food packaging offer mechanical protection, printability, and attractive appearance and barrier properties against oxygen, carbon dioxide, aromas, water vapour, microbial action, and grease. Single-layer biopolymer films are not usually competitive when compared against synthetic films (Vartiainen et al., 2014). By multi-layer structures the technical attributes can be significantly improved and the shelf life of the food item is prolonged. (Mihindukulasuriya and Lim, 2014; Vartiainen et al., 2014) However, multi-layer packaging can be blamed for high cost and difficult recycling of the material. The consumer may rather have bio-based biopolymer being next to the food item than not-so-healthy plastics.

Polyethylene, polypropylene, and fluoropolymers are today commonly used as grease barriers in packaging materials. The drawback of using fluoropolymers is the risk of accumulating the minor fractions of polytetrafluoroethylene into the fatty oil in the food (Begley et al., 2005; Whittaker et al., 2008). Package recycling reduces waste, but Suciu et al. (2013) describes how food packaging made by recycled materials contained contaminants like bisphenol, bis (2-ethylhexyl) phthalate, and nonylphenol monoethoxylate. (Suciu et al., 2013) Plenty of research is assigned in an area of natural fibre-reinforced (plastic) composites (Thamae and Bailie, 2008). Taking the idea further, a sensible option would be to entirely replace the synthetic polymers in grease barriers using native or modified polysaccharides, from wood or herbaceous plants (Kjellgren et al., 2006). Close to the ultimate material as food packaging would be one that is mechanically adequate, bio-based, biodegradable, economically and ethically feasible, as well as edible and health-promoting (Hansen and Plackett, 2008; Martins et al., 2012; Miller and Krochta, 1997). In food packaging there is a need for barriers against oxygen, aroma, carbon dioxide, and water and the packaging needs to prevent toxicological substances from being in contact with the food (Escalante et al., 2012; Johansson, 2011; Schmidt et al., 2013; Yaich et al., 2014).

There is generally a challenge in the exploitation of hydrophilic polysaccharides in barrier materials. For instance, chitosan coating on paper could not improve the water vapour barrier properties at all (Kjellgren et al., 2006; Kuusipalo and Lahtinen, 2005). Hartman et al. 2006 tackled this obstacle by etherifying the hemicellulose; GGM was hydrophobised with benzyl substitution and the derivative formed self-sufficient, transparent and firm films with rather good water repellence.(Hartman et al., 2006) However, other barrier properties are possible to obtain in straightforward manner. GGM and microfibrillated cellulose were plasticised with glycerol and showed promising properties as oxygen barrier in composite films. Mannan- and xylan-based films have been shown to possess good oxygen and grease barrier properties (Mikkonen and Tenkanen, 2012; Mikkonen et al., 2009, 2010). The oxygen permeability (OP) of hydroxyalkylated xylan was one third of that for a polyethylene terephthalate (PET) coating (Laine et al., 2013). Barrier attributes have been attempted by crosslinking GGM. GGM films have been cross-linked by ammonium zirconium carbonate and the film-forming ability was improved while the water uptake was reduced (Mikkonen et al., 2013). A rather unique approach, where GGM was cross-linked with laccase by utilising the naturally bound aromatic moieties, applied enzymes to increase the molar mass (Oinonen et al., 2013). The cross-linked material was then used for barrier films and the mechanical properties were significantly improved.

In order to make films solely of GGM, fairly high plasticiser content was required (Mikkonen et al., 2011). Non-modified GGM is hydrophilic and hygroscopic, but despite of that, plasticized GGM films have shown rather promising barrier attributes with low OP and moderate water resistance (Mikkonen et al., 2010). The OP values of various biopolymers are demonstrated in a Table 1.

Table 1. OP values of films. Arabinoxylan = AX, cationic polyethyleneimine = PEI, carboxymethyl cellulose = CMC, carboxymethylated microfibrillated cellulose = CM-MFC, polylactic acid = PLA, PHA= polyhydroxyalkanote

Substrate	**OP [(cm^3·µm)(m^2·kPa·d)]**	**Reference**
CMC-PEI on PLA	0.7	(Aulin et al., 2013)
NFC-PEI on PLA	0.3	(Aulin et al., 2013)
Xylan-NFC	0.2	(Hansen et al., 2012)
AX/GGM-NFC	1.2-1.7	(Stevanic et al., 2012)
CM-MFC	0.5	(Aulin et al., 2010)
GGM	2.0-6.8	(Hartman et al., 2006; Mikkonen et al., 2010)
NFC	0.2.2.5	(Aulin et al., 2010; Österberg et al., 2013)
PLA	150	(van Tuil et al., 2000)
PHA	160	(van Tuil et al., 2000)

The incorporation of nanofibrillated cellulose (NFC) into pullulan films improved their mechanical properties. The addition of glycerol into these NFC-pullulan films enhanced the flexibility and homogeneity of the films and also increased the Young's modulus and tensile strength even up to 8000% (Trovatti et al., 2012). About 80-85% of NFC within GGM and arabinoxylan hemicelluloses showed high mechanical, thermal, moisture sorption and excellent oxygen barrier properties (Stevanic et al., 2014).

The surface hydrophobicity of a material may be estimated by the CA of a water droplet deposited onto its surface. Hydrophobicity is achieved by lowering the surface energy, that is, the polar contribution to it, and by making adequate surface morphologies, which prevent water from spreading (Cunha and Gandini, 2010; Spiridon et al., 2013). In addition, water vapour transfer (WVTR) analysis is an efficient way to determine the rate of water transfer through the matrix. The varying analytical methods of the grease barrier measurements of biopolymer coatings and different conditions used with WVTR determinations make a comparison between studies rather challenging but still meaningful. et al. (2014) exhibited bilayer-coated papers using different combinations of proteins or polysaccharides with beeswax. The results with chitosan coating for a greaseproof paper were comparative to the grease barrier of commercial PET (Kjellgren et al., 2006). The room temperature modified T 507 cm-99 grease barrier test demonstrated zero penetration values for these 1-3% chitosan–beeswax coated papers. The grease barrier property was determined by TAPPI 454 with turpentine oil, where the maximum time of the test was 1800 s. The coat weights exceeding 5 g/m^2 had excellent grease barrier values, and the values had a strong correlation with the air permeance values. Their WVTR value was 53 g/m^2/d with 4.9 g/m^2 coating. Arabinoxylan films provided 100% barrier against sunflower oil for 48 h at 60 °C (Mikkonen et al., 2009). NFC films were grease proof for the measured time of 4 hours at 60 °C (Österberg et al., 2013). Chitosan was esterified with fatty acid chains, where interestingly a chitosan esterification took place on hydroxyl groups of C3 and C6 but not on amino groups (Bordenave et al., 2010). The comparison was made between the coatings of a chitosan-palmitic acid blend and palmitic acid esters of a chitosan-chitosan blend. Neither of them improved the WVTR values from 170-240 g/m^2/24 h, but they did improve the liquid water sensitivity determined by water contact angle measurements. Another approach was to combine an inorganic layer with the organic layer: atomic layer deposited ultrathin (25 nm) Al_2O_3 double coating on polylactic acid (PLA) films improved the water vapour barrier properties (Hirvikorpi, 2011; Kääriäinen et al., 2011). PET, PLA, low density polyethylene (LDPE), and polypropylene (PP) extrusion coated paper material had values of 19, 72, 5, and 4 g/m^2/24 h, respectively with the 25 g/m^2 coating weight. Upon normalising the results to the 10 g/m^2 coating weight, the LDPE and PP were more, PET was in the same range, and crucially PLA and PHA had much lower ability to resist water vapour.

3.3.5. Other potential applications with GGM hemicelluloses

Recently GGM has been considered as a highly potential raw material also for other than barrier functionalities. Quite a few efforts have been accomplished to alter the structure aiming towards to the specific applied property – structure relationship: Allyl functionalities were selectively introduced to the galactose unit of GGM by combining oxidation by galactose oxidase with an indium-mediated reaction (Leppänen et al., 2014). Block and grafted GGM derivatives with well-defined synthetic polymer chains were synthesised using controlled polymerisation techniques (Dax et al., 2013b; Voepel et al., 2009). Nonionic surfactants were synthesised from GGM with naturally occurring saturated fatty acids (Dax et al., 2013a). Carboxymethylated GGM functioned well as an emulsion stabilizer and increased the retention of fibrous material slightly (Xu et al., 2011). GGM and modified GGM also worked as wet-end controller in papermaking (Lindqvist et al., 2013; Xu et al., 2010). 2-hydroxyethylmethacrylate-GGM hydrogels have been applied for a controlled release of bovine serum albumin (Roos et al., 2008). GGM also acted as a carbohydrate source for probiotic bacteria (Polari et al., 2012). Sulphonation of GGM considerably enhanced the antithrombotic effect, which can be used therapeutically for prevention treatment of dangerous blood coagulation (Doliška et al., 2012). GGM was discovered to have potential as additives with immuno-potentiating and antioxidant properties e.g. in food products and pharmaceutical formulations (Ebringerová et al., 2008). Gel-like formation for controlled release of drugs have been built up by using GGM (Voepel et al., 2009). GGM was transesterified by glycidyl methacrylate to build hydrogels for arsenic and chromium removal from aqueous solutions (Dax et al., 2014).

3.3.6. This study

This project was carried out as a part of an industrial project (Future Biorefinery Joint Research Programme, Fibic Ltd. and TEKES), which had a target to establish cellulose and hemicellulose-based barriers for food packaging by tailored chemical synthetic approaches. However, I had the freedom of deciding the methods and applications within the hemicellulose functionality in a biorefinery concept. The study focused on derivatisation of GGM. Particular attention was put on the describing the chemical structure of the GGM derivatives. Furthermore, functionalised GGM were studied for barrier applications on cartonboard and on NFC-GGM biocomposite films.

4. Experimental

4.1. Materials

Two GGMs with different molar mass values were obtained. Low-molar-mass GGM (LMW-GGM) was obtained by hot-water extraction, which can be refined more efficient by adjusting the pH by on-line measurement and pH-buffer extraction (Kilpeläinen et al., 2013; Kilpeläinen et al., 2014; Krogell et al., 2013; Rissanen et al., 2014; Song et al., 2008). The concentrate was further filtrated with a hydrophilic RC70PP regenerated cellulose acetate membrane (10 Da, Alfa Laval) resulting in a 9 kg/mol GGM isolate; 17 % water dispersion of GGM was precipitated (purified) with 90 % ethanol followed by filtration. The filtrate was still washed with acetone and methyl *tert*-butyl ether. High-molar-mass GGM was obtained from a thermomechanical pulp mill process water (Willför et al., 2003b). The water was ultrafiltrated to obtain the GGM concentrate, and the concentrate was further spray-dried (Xu et al. 2009). The product was washed with 90 % ethanol and filtrated. The molar mass (M_w) of (high-molar-mass) GGM was 50 kg/mol. Stora Enso provided Cupforma Classic Natura 210 cartonboards for testing. The dispersion of NFC was prepared from softwood sulphite pulp (Nordic Pulp and Paper, Sweden) by subjecting to an enzymatic pretreatment according to (Henriksson et al., 2007).

The Norway spruce pulp pretreated by enzymatic treatment was disintegrated by passing through a microfluidizer (Microfluidics Ind., USA) connected to series of chambers with diameters of 400, 200 and 100 µm for several times (Henriksson et al., 2008). The NFC dispersion was diluted with deionized (DI) water to obtain a final concentration of 0.2 wt-% before the film formation.

4.2. Methods

4.2.1. Etherification of GGM (I)

GGM (2 g, 12 mmol) was dispersed in water (15-30 mL) and 1 M NaOH (9–14 mL) was added under magnetic stirring in round-bottom flask. Alternately GGM was dispersed in 20-30 wt-% of THF or DMSO/water. The dispersion was heated to 50 °C under magnetic stirring and then ETA (0.34–14 mL, 3-48 mmol) was added. The reaction was quenched by neutralising the reaction mixture with acetic acid or 1 M HCl. The cationic ether of GGM (Cat-GGM) purified was washed by precipitation using ethanol.

4.2.2. Acetylation of Cat-GGM (I)

Cat19-GGM (6 g, 28 mmol) was suspended in acetic anhydride (80 mL) and pyridine (5 mL) in a round-bottom flask under magnetic stirring. The reaction mixture was heated to 70 °C for 2.5 h. The product was washed with 90% acetone three times and dialysed with a 12–14 kDa cut-off dialysis tube.

4.2.3. Esterification of GGM (II-IV)

GGM or LMW-GGM was added to DMF and pyridine under magnetic stirring in a round-bottomed flask (I-IV). The dispersion was heated to 40-130 °C. The benzoic, butyric, phthalic or succinic anhydride was then added to the dispersion. After a certain reaction time, the product dispersion was washed with organic solvent-water blend, centrifuged, filtrated or dialysed against deionised water.

4.2.4. DS and acetyl determination by RP-HPLC (II-III)

The benzoyl, butyryl and phthalic content of GGM and modified GGM were determined by analysing the corresponding acid of the hydrolysate of modified GGMs. The defined weight of GGM ester was added in 4 mL of 0.5 M NaOH 50% MeOH in a pear shaped flask, 2-hydroxybenzoic acid was added as the internal standard. The solution was kept at 70 °C for 5 h and then for 18 hours at ambient temperature, being shaken manually during the hydrolysis. Samples were acidified to pH 3.2 with 0.5 M HCl and filtered with 0.2 Im PTFE syringe filters prior to HPLC analysis.

The gradient for GGM-Bu and GGM-Bz hydrolysates consisted of mobile phase A: 0.1% AcOH in 22% MeOH/H_2O and mobile phase B: 0.1% AcOH in MeOH. Elution profile of mobile phase A: 98% from 0 to 5 min, 98 to 45%, from 5 to 20 min, 45% from 20 to 30 min, 45 to 98% from 30 to 35 min and 98% from 35 to 45 min. Calibration was carried out with the corresponding acids: benzoic, butyric and phthalic acid (in 50% MeOH). The isocratic elution For GGM-Ph hydrolysate consisted of the mobile-phase 17.5 % MeOH/H_2O with 0.02 M KH_2PO_4 buffer. The pH of the eluent was adjusted to 2.49 with orthophosphoric acid. With the GGM ester hydrolysates the RP-HPLC instrument setup consisted of with an Agilent Technologies 1260 Infinity series chromatograph including an Agilent G131D DAD UV-Vis detector. With the GGM-Bz and GGM-Bu hydrolysates the column was a Phenomenex Gemini 5 µ C18 and for GGM-Ph hydrolysates the column was a Phenomenex Kinetex 2.6 µm, C18.

The acetyl content of native and modified GGM was determined by RP-HPLC as acetic acid content after alkaline hydrolysis. Alkaline hydrolysis of the defined amount of GGM ester and GGM was carried out in 10% MeOH and 0.5 M NaOH (5 mL) for 5 h at 70 °C. Samples were acidified with dilute

H_3PO_4 to pH 2.9 and the volume of the acid was recorded. Isocratic elution was carried out with 20 mmol KH_2PO_4. Acetic acid (0.04–0.08 mg/mL) was used as external standard for calibration. The column of RP-HPLC was Phenomenex Synergi 4 µ hydro-RP C18.

4.2.5. FTIR (I)

FTIR spectra were obtained on a Fourier transform infrared spectrophotometer (Bruker Vector 22) using KBr pellets containing 1 wt-% of a sample. 16 scans were accumulated with a resolution of 4 cm^{-1}, at 400–4000 cm^{-1}.

4.2.6. Matrix-assisted laser desorption/ionisation time-of-flight mass spectrometer (MALDI-TOF-MS) (I,III)

MALDI-TOF-MS analysis was performed with a SAI LT3 Plus MALDI-TOF mass spectrometer (SAI Ltd., Manchester, United Kingdom) equipped with a nitrogen laser of 337 nm and operated inpositive ion mode (Xu et al., 2012). MALDI-TOF-MS samples were prepared by mixing 0.5 µL of sample solution with 0.5 µL of matrix solution (10 mg/mL2,5-dihydroxybenzoic acid in acetone) on the MALDI-TOF-plate followed by drying under a stream of air. The GGM-Ph or Cat-GGM was enzymatically digested prior to the analysis, so that the substrate was dispersed in acetone (1–10 mg/mL), and an endo-1,4-mannanase was added. The solutions were stirred at room temperature for 48 h, and were then heated in boiling water for 10 min to inactivate the enzymes.

4.2.7. NMR (I-IV)

NMR spectra were recorded using a Bruker Advance NMR spectrometers instrument operating at 600.13 MHz (^{1}H: 600.13 MHz, ^{13}C: 150.90). DMSO-d_6 (I-IV) or D_2O (I) was used as solvent. The results are expressed in ppm scale using DMSO (I-IV) or 4,4-dimethyl-4-silapentane-1-sulfonic acid (I) as the internal standard. The probe temperature during the experiments was kept at 50 °C. DMSO-d_6 was used as the solvent. The samples were dissolved in DMSO-d_6 (140 mg/mL) and run at 50 °C. A 15-s pulse delay (D1) and an inverse-gated decoupling pulse sequence were used for quantitative ^{13}C measurements and 2-s pulse delay (D1) for ^{13}C measurements and 1-s pulse delay (D1) for ^{1}H measurement.

Also Distortionless Enhancement by Polarisation Transfer with 135° pulse angle (DEPT-135) (I), CH_2 edited HSQC (I), HSQC (II), and ^{1}H NMR (I, IV) were used. A 15 s pulse delay (d1) and an inverse-gated decoupling pulse sequence were used for quantitative ^{13}C measurements, and 2 s pulse delay (d1) for (non-quantitative) ^{13}C measurements. A 1 s pulse delay (d1) was used for ^{1}H, as well as, DEPT-135 and CH_2 edited HSQC measurements. About 15 000 scans were collected for quantitative ^{13}C NMR and 24 000 for ^{13}C NMR, 16 for ^{1}H NMR, and 128 for CH_2 edited HSQC. HSQC spectra were optimised for 145 Hz one bond and for 10 Hz long-range ^{1}H – ^{13}C coupling constants.

4.2.8. Elemental analysis of nitrogen (I)

The nitrogen content of Cat-GGM was analysed with a CHN LECOCHN-1000 elemental analyser at the Finnish Forest Research Institute. The blank sample of raw GGM was treated with 1.5% NaOH for 6 h at 50 °C and washed with ethanol. It contained 0.17 wt-% of nitrogen, probably originating from protein residues in wood. This was taken into account in determination of DS with N-analysis. The nitrogen wt-% of the elemental analysis (EA) was used to deduce the DS (Bigand et al., 2011) in the following way:

$$DS^{EA} = \frac{M_{man} \times N\%}{M_N \times 100 - M_{func} \times N\%}$$

where M_{man} is the molar mass of the mannose, N% equals nitrogen wt-% of the sample, M_N is the molar mass of nitrogen and M_{func} is the molar mass eight of the functional group, 151.6 g/mol.

4.2.9. Thermal analysis (I-II)

The glass transition temperature (T_g) was measured by differential scanning calorimetry in a range from 60 °C to 150 °C. T_g was taken from mid-point of the change in slope.

Thermal decomposition (thermogravimetric analysis, TGA) was measured with a Thermo Gravimetry/Differential Thermal Analyzer TG/DTA320 Seiko Instruments at VTT, Tampere, Finland. About 3 mg of sample was heated from 25 °C to 600 °C at 10 °C/min heating rate under argon flow.

4.2.10. Polyelectrolyte titration (I)

Polyelectrolyte titration with a particle charge detector can for instance be used to determine anionic charge in humic substances (Tan et al., 2011). Adsorption of cationic polyelectrolytes onto anionic polyelectrolytes is affected by various factors like salt residues in the dispersion, as well as molar mass and functional group properties of the polyelectrolytes (Böckenhoff and Fischer, 2001; Farris et al., 2012; Lundström-Hämälä et al., 2010). Charge density of cationised GGM was measured with Mütek Particle charge detector −0.3. Cat-GGM (0.1 g) was suspended in water and 0.001 M potassium polyvinyl sulphate was added until reaching the zero point. The titration was repeated two times and the average value was used in calculation. The results from polyelectrolyte titration are expressed as eqv./g (mol/g). Charge density of the single charged group can be converted to nitrogen wt-%, from which we can deduce DS in the following way:

$$DS^{PT} = \frac{M_{man} \times N\%}{M_N \times 100 - M_{func} \times N\%}$$

Where M_{man} is the molar mass of the mannose, N% equals nitrogen wt-% of the sample, M_N is the molar mass of nitrogen and M_{func} is the molar mass of the functional group (without a chloride ion), 116.2 g/mol. The formula is derived from the formula of DS^{EA} described in a chapter 4.2.8.

4.2.11. Molar mass (I-II)

Molar mass determination with multi-angle-laser-light scattering and refractive index (MALLS-RI) detectors was carried out in water for Cat-GGM or in DMSO for the GGM or LMW-GGM esters.

The weight-average molar mass (M_w) was determined by size-exclusion chromatography (SEC) in on-line combination with a MALLS instrument (miniDAWN, Wyatt Technology, Santa Barbara, USA, (0= 690 nm) and a RI detector (Shimadzu Corporation, Japan). The eluent was 0.1 M $NaNO_3$ solution for the GGM ethers and 0.05 M LiBr DMSO for the GGM esters. Astra software (Wyatt Technology, Santa Barbara, USA) was used to interpret the data.

It is crucial to know the exact value of d*n*/d*c* (refractive index increment) with SEC-MALLS analysis, because the system has refractive index detection and the concentration of the sample is not known. However, the determinations are seldom carried out but values of literature to resembling polymers are often used. In this study, the d*n*/d*c* value of 0.150 was used (Michielsen, 1999) for GGM and GGM ethers in water (I) and self-determined value in DMSO with LiBr for GGM-Bz , GGM-Bu in DMSO (II). The d*n*/d*c* value of 0.073 was determined with a differential refractometer (k = 632.8 nm) in the concentration interval of 2–20 mg/mL for the sample of GGM-Bz7 in 0.05 M LiBr DMSO at ambient temperature. The accurate concentration of stock solution of GGM-Bz7 was determined with ^{1}H NMR by measuring the aromatic signals against the molar quantity of 2-propanol. 44% of the dry mass where in a liquid phase according to the determination.

4.2.12. Solubility (I-IV)

The solubility of GGM and GGM derivatives in water and in organic solvents was measured gravimetrically at ambient temperature after centrifugation in 1% (w/w) concentration (Figure 3).

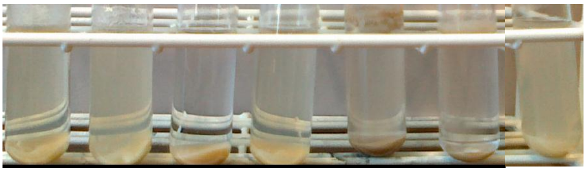

Figure 3. Testing the solubility in water with GGM esters.

4.2.13. Preparation of NFC films (IV)

The diluted NFC dispersion was mixed at 8000 rpm using an Ultra Turrax mixer (IKA, T25 Digital). The NFC film was subsequently prepared by filtration on a fine membrane and dried using Rapid Köthen Sheet Former, according to a previously reported method for the nanopaper (Sehaqui et al., 2011).

4.2.14. Preparation of NFC-GGM composite films (IV)

Aqueous dispersion of 0.1 wt-% LMW-GGM was prepared with de-ionised water. The LMW-GGM dispersion was heated shortly at 90 °C to improve solubility of LMW-GGM prior to mixing with the NFC dispersion. Moreover, the GGM dispersion was filtered through a fine nylon cloth in order to remove the water-insoluble fraction in advance. A thorough mixing was performed on the mixture of NFC and LMW-GGM dispersions at 90 °C for 4 h. The NFC-GGM film was further prepared by filtration and drying similarly to the NFC reference film. During filtration, a major portion of GGM was lost through the fine membrane. The LMW-GGM content was determined by weighing the left-over LMW-GGM. The NFC-GGM film with a final LMW-GGM content of 5.5 wt% was successfully prepared and selected for the further coating study.

4.2.15. Coating of the films (IV)

15 wt-% water dispersion of LMW-GGM or GGM-Su1 or 15 wt-% ethanol dispersion of GGM-Su2 with 15 wt-% of sorbitol was prepared for the coating of the films. The coating was performed with a K-control (bar) coater. The wet coating was dried under UV lamp for ~6 seconds and then placed between two polyamide meshes with 36.5 µm pore size followed by two plotting papers and plastic boards with 4.5 kg weight on a top. The entity was put into a vacuum oven at 40 °C for the further 18 h.

4.2.16. Scanning electron microscopy (III-IV)

The cross-section surfaces of the films were viewed with scanning electron microscopy (SEM). An UltraDry Silicon Drift Detector was used. The SEM was operated under high vacuum, using secondary electron-imaging mode. The magnification of the image corresponds to a Polaroid 545 print with the image size of 8.9 X 11.4 cm.

4.2.17. Grease barrier testing (III-IV)

Grease barrier testing of the coated cartonboards (III) was optimized from the optical method of Bollström et al. (2012) and carried out at ambient temperature at 22–30 % relative humidity (R.H.) (Bollström et al., 2012). The cartonboard and cylinder were placed onto the prism, and 1.5 mL of Oil Red O coloured rapeseed oil was put into the cylinder hole with 8 mm diameter. Three samples of each kind of cartonboard were measured. The degree of penetration was quantified via image analysis (pixel count) with image software of the obtained images as function of time. The value of 0.1 % oil penetration was determined; 72 h was the maximum measuring time, two measurements with GGM-Ph (2.4 g/m^2) and one with GGM-Bz (2.4 g/ m^2) out of three were stopped at 72 h without any grease penetration; thus, the determined value is an underestimation. The grease barriers over the 10 g/m^2 coatings with olive oil were tested with the ASTM F119-82 method, thus at 50 % R.H. at 23 °C.

Grease barriers of the NFC-GGM-GGM-Su films (IV) were determined using at modified method of the previously described one. Food-grade rapeseed oil was applied on the films. 100 mL of oil was coloured with 1 g of 1-[[2-methyl-4-[(2-methylphenyl)azo]phenyl]azo]-2-naphthalenol (solvent red 24). Surplus of oil was put into the cylinder hole. Grease barrier was determined with a method of where cylinder on top of the film was filled with coloured rapeseed oil, and the sorption paper was underneath. The films had been conditioned for 24 h at 23 °C and at 50 % RH prior to testing. The testing was carried out in a chamber at elevated temperatures and R.H.

4.2.18. Dynamic mechanical analysis (DMA) in humidity mode (IV)

Dynamic mechanical analysis (DMA) on NFC-GGM films was carried out with a Q800 dynamic mechanical analyser (TA Instruments, USA). The analysis was performed in tensile mode using a controlled R.H. accessory. The storage moduli (E_0) of NFC-GGM films were recorded as a function of time at 30 ^{o}C. Samples were initially equilibrated at 0 % R.H. and 30 ^{o}C. The DMA scan was performed in a stepwise manner at R.H. values of 0, 50, 90 % and once again at 0 % to record the extent of material recovery. Each humidity level was sustained for 300 min. Three parallel specimens were measured from each sample to calculate the average storage modulus at different R.H. values after 300 min equilibration.

4.2.19. Oxygen permeability and oxygen transmission rate

The oxygen transmission rate (OTR) of the films was measured using an OP analyser with a coulometric sensor (M8001; Systech Illinois, Oxfordshire, UK). The film was exposed to 100 % oxygen on one side and to oxygen-free nitrogen on the other side for the overnight measurement. The OP was calculated by multiplying the OTR value by the thickness of the film and dividing it by the oxygen gas partial pressure difference between the two sides of the film. The measurements were carried out at 23 ^{o}C, normal atmospheric pressure, and at 50 % R.H. The specimen area was 5 cm^2 and the thickness of the film was measured before analysis at five points with a micrometer at 1 µm precision. The OP was determined in duplicates.

4.2.20. Water contact angle (IV)

CA measurements were carried out with a KSV CAM 200 (later Biolin Scientific) optical goniometer and One Attension Theta1.4 software. 18.2 MΩ type-1 deionized distilled water was used. Three microliter drops were released onto the sample surface with the sessile drop measurement method. At least five different measurements per specimen were carried out.

4.2.21. Water vapour transmission (WVTR) (III)

WVTR of cartonboards was evaluated using the NF ISO 2528 method. An aluminium cup with a dried $CaCl_2$ desiccant was sealed by the test cartonboard (0.005 m^2). The edges were covered with wax (Figure 4). The duplicate samples were placed in the conditioning room at 23 °C in 50 % R.H. The weight of the cup was recorded in intervals of five times in 2 days.

Figure 4. Pouring wax on the cartonboard edges for WVTR determination.

5. Results and discussion

5.1. An overview of the chemical modification of GGM (I-IV)

By chemical modification of polysaccharides we can obtain new functionalities. These novel derivatives can be considered as tools to be used later in various applications. A scope of this work was to esterify GGM to fit to the demand of functioning as barrier material biocomposites applied in food packaging. Additionally, cationised GGM ether can potentially be applied as polyelectrolyte (multi)layering for packaging applications, biosensors, electronic devices, and printing applications on films and paper (Leppänen et al., 2013; Mielonen et al., 2015; Schoeler et al., 2006).

The challenge for the use of hemicelluloses for material applications is their hydrophilicity. To overcome this, we aimed to make GGM hydrophobic by chemical means to be used for packaging applications. Controlled methods of esterification and cationisation in water and in water with THF or DMSO were established. Various analytical tools were used to characterise the GGM derivatives and compare the degree of substitution (DS) and to acquire parallel proof of the structural characteristics. No protecting groups were used in the one-step reactions with GGM; the molar yields can be high in comparison to the multistep reactions e.g. in non-polymeric carbohydrate synthesis (Sail and Kováč, 2012).

$$DS = \frac{the\ average\ number\ of\ substituents}{sugar\ unit}$$

$$RE = \frac{eqv. of\ reagent}{DS}$$

One of the aims was to examine the reaction parameters of GGM etherification with cationic groups and esterification with non-polar moieties and perform characterisation of the products. The cationic group possesses the nonpolar methyl group, methylene and methine bridges, ammonium cation, and the hydroxyl group; hence we can presume an overall an amphiphilic character of the functional group. The characterisation was focusing on molar mass, DS, regional substitution on the hydroxyl group of C6 in relation to C2 and C3, RE, solubility to various solvents, and thermal properties.

Several analytical techniques were used to determine DS not only for the sake of overall accuracy and certainty but also to discover the most fluent and justified technique depending on the number of samples and available facilities. Moreover, various aspects of the chemical and physico-chemical structure can be discovered with multiple analytical methods. One of those is NMR, which is a fundamental method for characterisation of the chemical structure (Heinze et al., 2006), and which was an important tool also in this work.

Modification of GGM is relatively easy in comparison to modification of cellulose; GGM with intact acetyl groups is soluble or well soluble (Willför et al., 2003a) in water at 23 °C and in DMF and in DMSO upon heating (I-IV). The synthesised GGM derivative can be dispersible or soluble to water, ethanol, DMSO, or DMF depending on the DS (Figure 5). The ultimate objective was to use GGM derivatives for material applications. The introduced functional groups bonded covalently with the hydroxyl groups of GGM. However, upon using GGM derivatives in coatings and composites, e.g. dipole-dipole interactions including hydrogen bonding, Van der Vaal forces and hydrophobic interactions may have taken place. A scope of this work was to esterify GGM to fit to the demand of barrier material as part of biocomposites or coatings.

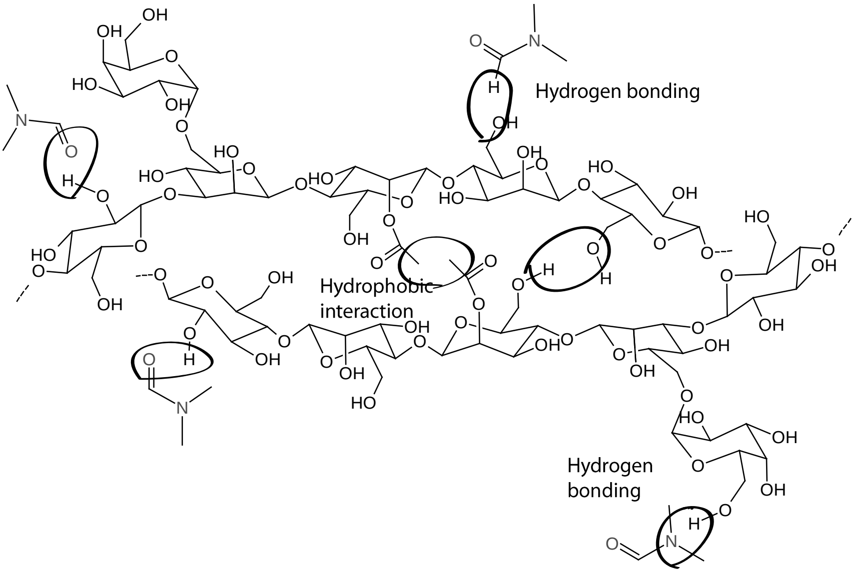

Figure 5. Hypothetical intermolecular interactions of GGM and dimethylformamide (DMF), which was the solvent in esterifications of GGM. The circles point out dipole-dipole interaction of hydrogen bonding and hydrophobic interaction. DMF as aprotic solvent does not donate protons (H+).

5.2. Cationic etherification of GGM and acetylation of GGM ether (I)

5.2.1. An overview of the reactions

Cationisation of GGM was carried out heterogeneously in water, in water with THF, or in water with DMSO in alkaline conditions with the common reagent of ETA (Figure 6). Particular attention was paid to accomplish the structural characterisation from different perspectives. NMR, polyelectrolyte titration (PT), and elemental analysis (EA) methods were used for DS determination. NMR, MALDI-TOF-MS, SEC-MALLS and FTIR were used as a tool for structural characterisation. Furthermore, the effect of the DS value on decomposition temperature (T_g) and T_d was examined. The significance of the organic solvent to the reaction output was studied with miscible solvent blends of THF-water and DMSO-water.

The cationised product was neutralised and purified in ethanol. The quantity of sodium hydroxide (0.3–4 wt-% of solvent), reagent (0.05–4 eqv./sugar unit), reaction temperature (30–60 °C), and reaction time (3–24 h) were altered to examine their effect of that on the RE, DS, and molar mass (Table 2). The *O*-acetyl groups of GGM were hydrolysed in alkaline water during the cationisation. GGM lost its water solubility upon losing its acetyl groups when cationised. We thus carried out re-acetylation to hydrophobised the Cat-GGM.

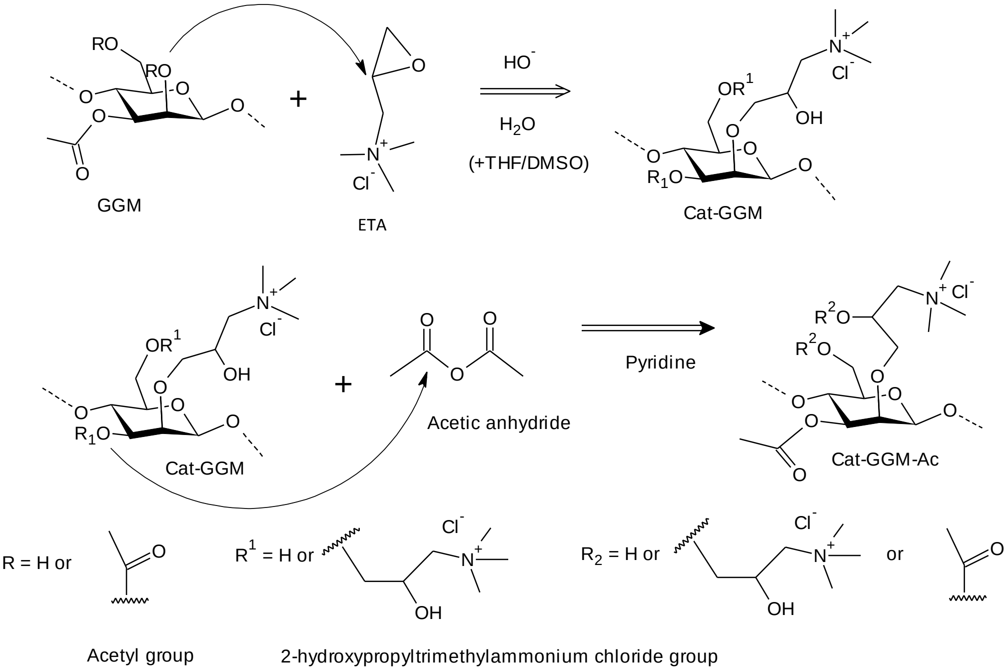

Figure 6. Etherification of GGM with a cationic group and acetylation of cationised GGM (I). ETA = 2,3-epoxypropyltrimethylammonium chloride.

An interesting feature was discovered in the reaction pattern; the reaction with the cationic moiety did not solely occur at the hydroxyls of the sugar backbone, but may have also occurred at the hydroxyl group of C8 of the cationised group (Figure 6). The issue is approached by the NMR analysis at Section 5.2.6. The highly strained three-carbon ring-structure of ETA was susceptible to attack of nucleophiles. Unfortunately also hydroxyl ions may have opened up the strained epoxy ring and hence decreased the quantity of the reagent (Bendoraitiene et al., 2006). The highest DS were achieved with large amount of reagent, with high sodium hydroxyde concentration, and having THF in the solvent (Cat23-GGM, Cat24-GGM, Table 2). The temperature increment from 30 to 50 °C with 0.8 wt-% of NaOH and with 1 eqv. of ETA increased the DS from 0.14 to 0.23 (Cat6-GGM and Cat8-GGM).

Table 2. Reaction parameters and analysis results of cationised GGM (Cat-GGM).

Cat-GGM	**Wt-% NaOH/ solvent**	**Eqv.of ETA**	**Wt-% of THF or DMSO in H_2O**	**Reac-tion time [h]**	**T [°C]**	**DS**		**RE-%**	**Molar mass [kg/mol]**
						EA	PT / NMR		
1	0.30	0.25	n.d.	6	50	0.023	n.d.	9	23.8
2	0.30	0.5	n.d.	6	50	0.034	n.d.	7	23.4
3	0.30	2	n.d.	6	50	0.12	n.d.	6	n.d.
4	0.30	1.5	49^{DMSO}	6	50	0.26	n.d.	18	18.3
5	0.36	1	n.d.	6	50	0.15	n.d.	15	22.7
6	0.78	1	n.d.	6	30	0.14	n.d.	14	22.5
7	0.78	1	n.d.	3	50	0.21	0.21^{PT} 0.19^{NMR}	21	21.3
8	0.78	1	n.d.	6	50	0.23	n.d.	23	19.2
9	0.78	2	25^{THF}	6	50	0.27	n.d.	13	20.0
10	0.90	1.5	n.d.	3	60	0.28	n.d.	19	16.3
11	0.90	1.5	30^{THF}	3	60	0.38	n.d.	26	19.0
13	1.2	1	20^{THF}	6	50	0.19	0.14^{PT}	19	24.2
14	1.2	4	25^{THF}	6	50	0.44	n.d.	10	16
15	1.2	6	25^{THF}	6	50	0.63	0.63^{PT}	11	n.d.
16	1.3	6	n.d.	24	50	0.58	0.62^{PT}	10	13.0
17	1.5	0.05	n.d.	6	50	0.022	n.d.	43	n.d.
18	1.5	0.1	n.d.	6	50	0.036	n.d.	36	15.7
19	1.5	1	n.d.	6	50	0.25	0.20^{PT}	25	*17.6*
20	1.5	1	n.d.	24	50	0.24	0.25^{PT}	24	*15.4*
21	1.5	2	n.d.	24	50	0.39	0.39^{PT}	19	14.8
22	2.0	1	n.d.	6	50	0.25	0.19^{PT}	25	19.4
23	2.1	6	25^{THF}	24	50	0.89	0.94^{PT} 1.13^{NMR}	15	9.3
24	3.1	6	25^{THF}	24	50	0.77	0.77^{PT}	13	9.0
25	4.0	1	n.d.	6	50	0.18	0.12^{PT}	18	17.6

5.2.2. Acetylation of GGM ether

Increased hydrophobicity and possible branching of the cationised acetylated GGM (Cat-GGM-Ac) over GGM and Cat-GGM renders further potential for film and coating applications (Figure 6). We carried out re-acetylation for Cat19-GGM (DS 0.25) with an excess of acetic anhydride and pyridine (Figure 6) according to the acetylation method of GGM by Xu et al., 2010 Acetylation was confirmed with NMR and FTIR. Acetyl groups are essential for water solubility in native GGM; however, they did not make Cat-GGM water-soluble but rather hydrophobic. The water solubility of Cat-GGM-Ac was 20% while Cat-GGM with DS 0.39 had value of 91%. Rather viscous appearance of Cat-GGM-Ac as solution in DMSO may refer to high degree of branching.

5.2.3. Characterisation of the cationic GGM ether and acetylated cationic GGM ether

The characterisation was carried out by FTIR to assign the fingerprinting of N-C, CH_2, and acetyl groups. By NMR and MALDI-TOF-MS we obtained the general verification of the product with a few aspects of the substitution pattern. By MALDI-TOF-MS we can perform accurate mass analysis also with large molecules (Gatenholm and Tenkanen, 2004). NMR gave proof of the product of the GGM with the cationic group. FTIR complemented with the evidence of N-C bonding. The polyelectrolyte titration and elemental analysis rendered alternative ways to determine DS. Characterisation of GGM derivatives in general is discussed in the chapter 5.4.

5.2.4. FTIR

The FTIR spectra of Cat24-GGM, Cat-GGM-Ac, and unmodified GGM are shown in Figure 7, where the band at 2930 cm^{-1} corresponds to CH_2 vibrations. The distinguished band of carbonyl stretching of acetyl groups at ~1740 cm is significant for the Cat-GGM-Ac, while the band is smaller for unmodified GGM and it is absent for Cat23-GGM. The band at 1480 cm^{-1} for Cat24-GGM indicate N-C bonding (Bigand et al., 2011; Pigorsch, 2009; Yu et al., 2007). The band at about 900 cm^{-1} is assigned to the glycosidic linkage (Xu et al., 2010). A band at ~3400 cm^{-1} does not indicate only hydroxyl stretching but possibly also water residues.

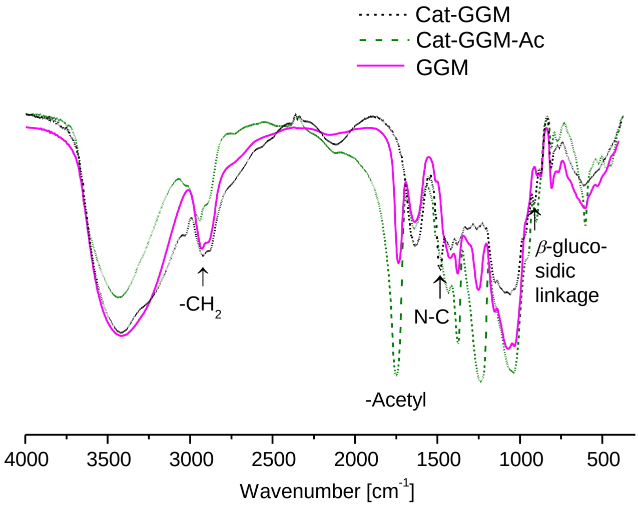

Figure 7. FTIR spectra of GGM, Cat23-GGM, and Cat-GGM-Ac.

5.2.5. MALDI-TOF-MS

With MALDI-TOF-MS, the main products of enzymatic hydrolysis were assigned to the GGM oligomers with the cationic group as the substituent. An *m/z* increment of 116 corresponds to the [O-(2-hydroxy-3-methylammonium)propyl]+ (=Amm) residue. Other distinguished cationised oligomers were with additional one and two O-(2-oxo)propyl (=OPU) groups by their consequent *m/z* increments of 56. The oxypropyl units (OPU) do not appear as an original substituent in Cat-GGM but have been formed from MALDI during the actual laser desorption/ionisation. The presence of the OPR units and the absence of multiple cations may indicate that the GGM oligomers with multiple cationic groups had undergone elimination of the trimethylammonium group during laser desorption/ionisation to their trimethylammonium residues until only one cationic trimethylammonium was left. The structures of the oligosaccharides with amm+ and OPR units identifying using MALDI are illustrated in Figure 8. Multi-reaction in the same sugar unit in the GGM backbone can be observed by the signal at m/z = 570.2 that has two sugar units and three functional units. The oligosaccharide pattern (observed after MALDI fragmentation) with repeating mono- and multiple cationised oligosaccharides with increasing sugar content (2-6 sugar units) indicates the heterogeneous distribution of the cationised groups within the GGM backbone.

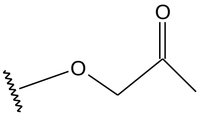

OPU

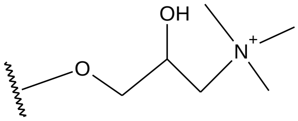

Amm

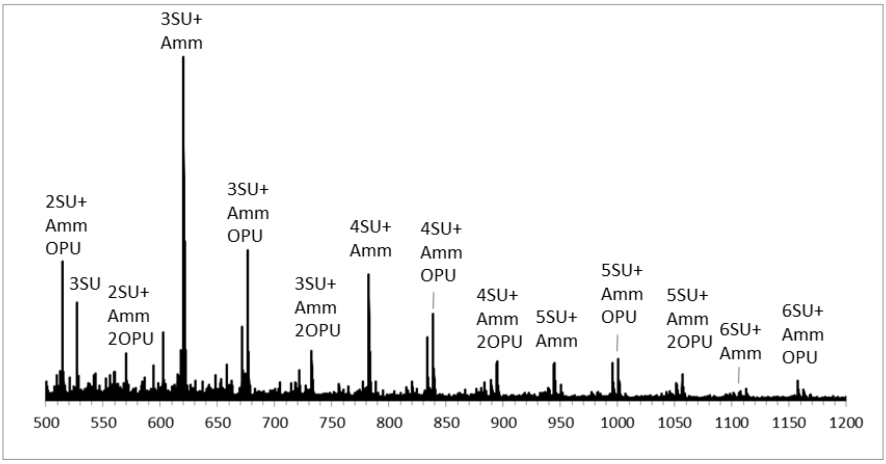

Figure 8. MALDI-TOF-MS spectrum of Cat8-GGM. O-(2-hydroxy-3-methylammonium)propyl is marked as [Amm], oxypropyl units as [OP] and sugar unit as [SU].

5.2.6. NMR

GGM esters was analysed with NMR to find out the overall chemical structure. However, plenty of overlapping of the signals of carbons C2-C6 (δ = 61-80 ppm) in ^{13}C NMR and of the signals of protons H2-H6 (δ = 3.3-5.5 ppm) in ^{1}H NMR of the mannose, glucose, and galactose units of GGM make interpretation laborious regarding regioselectivity of the reaction. The GGM mixture includes also small amounts of other hemicelluloses, which include some arabinose and xylose units, as well as uronic acids. Furthermore, the signal of the proton at the root of the acetyl group is overlapping with the signals of the anomeric proton in ^{1}H NMR.

The structure and DS of Cat-GGM was determined with several NMR techniques including quantitative ^{13}C (Figures 9-10) and ^{1}H NMR (Figure 11), DEPT-135 (Figure 12) and CH_2 edited Heteronuclear Single Quantum Coherence (HSQC, Figure 13). The quantitative ^{13}C NMR spectrum of GGM was used as a reference. C10 at δ = 55.8 ppm and C8 at δ = 67.6 ppm had distinguished signals, which were not appearing in GGM (Figures 9-10). Signals of C10 of the cationic moiety can also be observed in ^{1}H NMR (Figure 11). The negative signals in DEPT-135 indicated the presence of CH_2 (Figure 12). However, the negative signal of C7 is rather small. The existence of the negative signal of C7 was further tested by CH_2 edited HSQC, where CH_2 signals (negative correlations) are distinguished from CH and CH_3 signals (positive correlations). This method enables the differentiation of overlapping carbon resonances by expanding the spectrum to the proton dimension. The C7 signal (δ ~ 75.8 ↔ 4.2 ppm, CH2 type) really overlaps with another carbon signal (δ ~ 75.8 ↔ 3.6 ppm, CH type) and thus restrains the C7 signal to appear rather small in the DEPT-135 spectrum. The total DS was determined by comparison of the integral value of C10 (three carbons) against the anomeric carbon signal of the quantitative ^{13}C NMR (Figure 10) (Hannuksela and Hervé du Penhoat, 2004). The approximate degree of substitution at C6 (Xu et al., 2011) was determined by measuring the decrease of the integral value of the non-reacted C6 signal (δ = 59–63 ppm) of the Cat-GGM in comparison to unreacted GGM (Figures 9-10). The results showed that about 22% of C6 were reacted for Cat24-GGM with DS 1.13.The reduced size of the C8 signal in proportion to DS (0.80- and 1.13, respectively) was split in two tops and thus suggested a possible diastereomeric reaction of the cationic moiety on the hydroxyl group of the cationic group on C8 (Figure 10).

Cat-GGM-Ac was possibly more branched than Cat-GGM and hence formed a highly viscous gel-like solution in DMSO-d_6. Due to this, low concentration had to be used for measurements and this caused high signal to noise ratio in ^{13}C NMR, which disturbed thorough quantitative determination of the acetyl groups. However, signals of $\underline{C}OCH_3$ and $CO\underline{C}H_3$ can be detected, indicating acetylation. CH_3 of the acetyl group was observed also in ^{1}H NMR (Figure 11). The appearance of CH_2 of C7 and C9 at DEPT-135 indicates the presence of a cationic moiety after acetylation. The acetyl groups did make Cat-GGM hydrophobic.

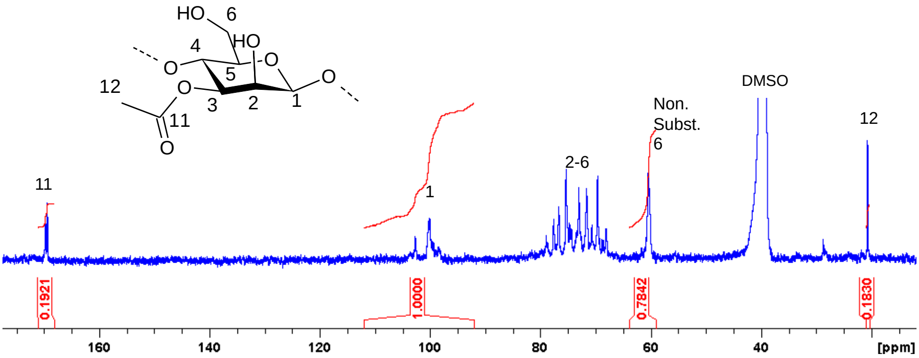

Figure 9. The quantitative ^{13}C NMR spectrum of GGM.

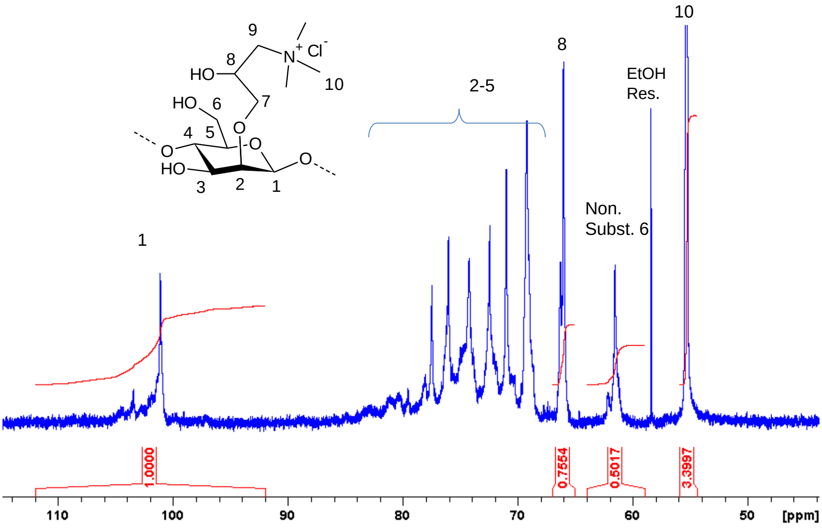

Figure 10. The quantitative ^{13}C NMR spectrum of Cat23-GGM.

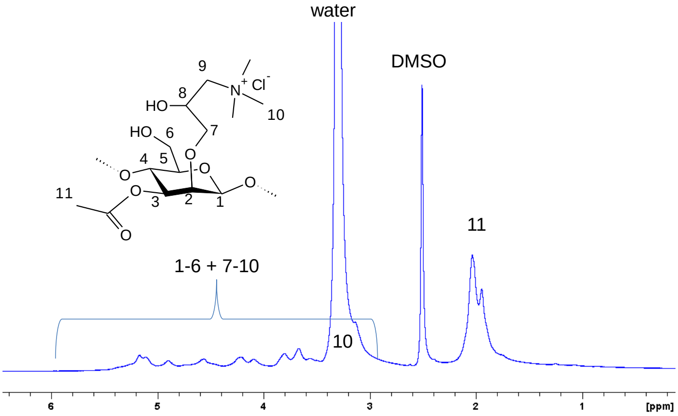

Figure 11. ^{1}H NMR spectrum of Cat-GGM-Ac

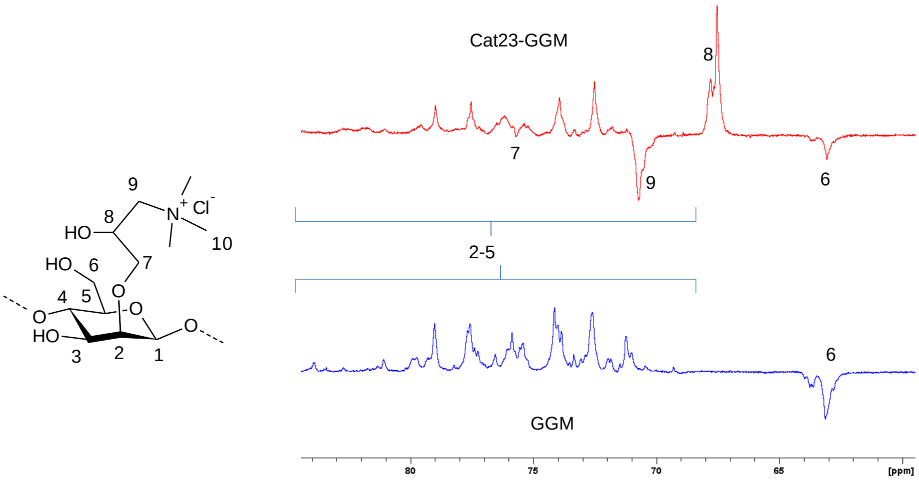

Figure 12. DEPT-135 NMR spectra of Cat23-GGM and GGM. CH_2 signals are negative while CH and CH_3 signals are positive.

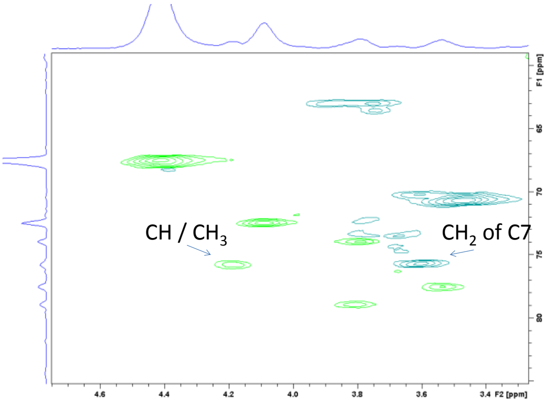

Figure 13. CH_2 edited HSQC of Cat23-GGM, where CH_2 has blue colour, CH and CH_3 have green colour. Protons at δ =3.6 ppm and δ = 4.2 ppm are partially overlapping in carbon spectrum at δ = 75.5 ppm for CH2 of C7. Therefore the negative signal of C7 in ^{13}C NMR on DEPT-135 is diminished.

5.2.7. Polyelectrolyte titration and elemental analysis

The DS from the charge density analysis versus DS from elemental analysis showed linear consistency (Figure 14). DS values under 0.25 determined with PT were lower than the ones with elemental analysis, which may arise from the acidic polymer fractions in GGM (Böckenhoff and Fischer, 2001; Xu et al., 2008). The DS value with PT was the same or even slightly higher for Cat-GGMs with high DS. The advantage of PT analysis is in larger series of samples, which could be analysed in less time consuming manner than by NMR or the elemental analysis. The DS was determined by quantitative

^{13}C NMR, EA and PT titration giving the values 1.13, 0.89, and 0.94 values for Cat23-GGM as an example of high DS and 0.19, 0.21, and 0.21 values for Cat7-GGM as an example of medium DS (Table 2). There was some difference in the values for the DS determined by NMR for Cat23-GGM, which can be elucidated by trapped solvent residues in the polymer, which are not affecting the NMR results.

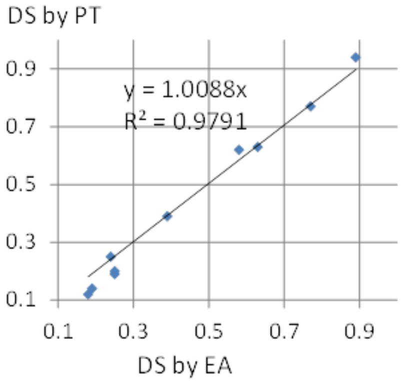

Figure 14. Correlation of DS results determined by elemental analysis with those determined by polyelectrolyte titration.

5.2.8. Molar mass

The effect of organic solvent, alkaline reaction media, and reaction time on the Cat-GGM decrease due to hydrolysis was studied. DMSO and THF in the reaction media and short reaction time had a beneficial effect on retaining the molar mass. High (2.1–3.1 wt-%) concentration of NaOH (Cat23-GGM and Cat24-GGM, Table 3) led to low molar mass of ~9 kg/mol.

5.2.9. Thermal characterisation

A low glass transition temperature makes the material less brittle and is thus an advantage in packaging (Mittal, 2011). T_g and T_d values of Cat-GGM, Cat-GGM-Ac and GGM are elucidated in Table 3. The thermograms of the DSC determinations showed endotherm signals indicating decreasing T_g temperatures with increasing DS of GGM. This was in accordance with the observation in a previous study for hexanoate and dilactates of pullulan (Donabedian and McCarthy, 1998), The thermograms of the Cat-GGM, GGM, and Cat-GGM-Ac did not show a crystalline melting behaviour as was the case for wood fibre-reinforced cross-linked starch composites (Duanmu et al., 2010; Jenkins and Donald, 1998; Thomas, 2001).

A raw material with a high T_d would tolerate exposures to high temperatures during the material processing. The thermal decomposition was analysed with TG/DTA, where decomposition temperatures $T_d^{10\%}$, and $T_d^{50\%}$ indicate 10% and 50% weight loss, respectively (Table 3). Acetyl groups and high DS of cationic groups give thermal stability to the polymer; Cat-GGM-Ac had higher T_d values in comparison to unmodified GGM and Cat-GGMs (I). The existence of the cationic group made no major difference, but Cat24-GGM of high DS provided lower T_d values than Cat6-GGM of low DS.

Table 3. $T_d^{10\%}$, and $T_d^{50\%}$ values indicating 10% and 50% weight loss, respectively, and T_g values. n.d. = not determined.

	Cat-GGM-Ac	Cat24-GGM	Cat15-GGM	Cat13-GGM	Cat6-GGM	GGM
DS	-	0.77	0.63	0.19	0.14	-
$T_d^{10\%}$ [°C]	262	241	n.d.	n.d.	249	241
$T_d^{50\%}$ [°C]	344	291	n.d.	n.d.	300	305
T_g [°C]	n.d.	n.d.	69	74	n.d.	86

5.3. Overview of the esterification of GGM (II-IV)

The object of the esterification was to make GGM hydrophobic and to enhance the oxygen, grease, and water barrier properties in film and coating applications on paper and board products. The level of hydrophobicity can be adjusted by different levels of DS. In order to make the films hydrophobic, the polarity of the GGM has to be reduced by diminishing the number of available hydrogen bonding sites of the hydroxyl groups. This can be done by introducing non-polar hydrocarbon moieties (Cunha and Gandini, 2010). Adjusting the reaction time, temperature, and the amount of reagent gave grounds to examine DS, RE, yield, solubility in various solvents, and suitability to barrier coating applications.

Benzoic, butyric, phthalic and succinic esters of GGM or LMW-GGM were synthesised (Figure 15). Though water would be the most feasible solvent in industrial scale, organic solvents were here appropriate for obtaining an effective synthesis.

5.3.1. The trends of the esterification (II-IV)

The reactions were carried out with anhydrides as reagent, DMF as solvent and pyridine as base (Figure 15). In the benzoylation and butyration reactions the leaving groups are benzoic acid and butyric acid, respectively. They are benign acids in comparison to the chlorinated side products from common reaction with acyl chlorides. A ring-opening of anhydrides occurred in the phthaloylation and succinylation reactions. The size of the reagent regulates the steric repulsion of the anhydride reagent to GGM. The trend of this can be evaluated indirectly by RE. The order of RE with three different esterifications were succiniliation > phthalaylation > benzoylation > butyration. The trend is in accordance with the size of reagent from small to large, with the exception of the butyration. Butyric anhydride itself caused a deficient solubility of GGM in DMF that made the reaction more heterogeneous. A critical factor obstructing the substitution of anhydrides can be the sterical hindrance caused by acetyl groups, whereas galactosyl side groups may hinder anhydrides reaching C6 positions of the backbone of mannose units of GGM. The organic solvent was appropriate to obtain effective reaction with anhydrides and in this work regional substitution was not in target. With butyration, different solvents for purification were also tested aiming at a sufficient yield. GGM was used in synthesis, unless stated that LMW-GGM was used.

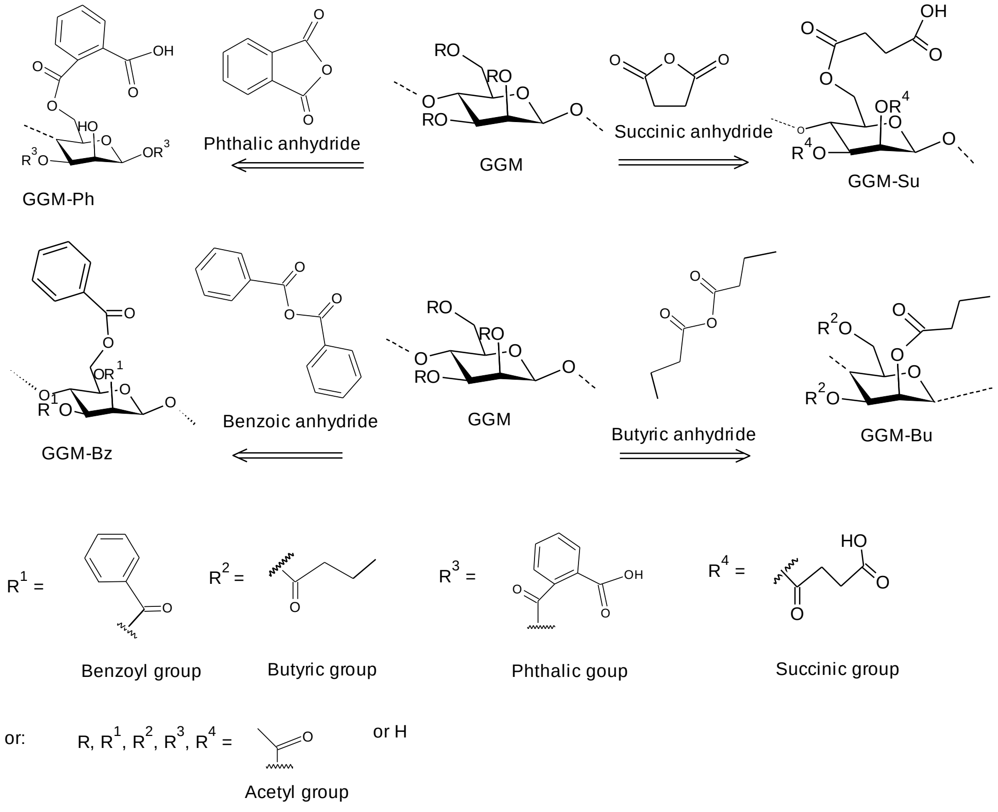

Figure 15. Benzoylation, butyration, phthaloylation and succinilation, and reactions with anhydrides.

The native acetyl groups remained mostly intact after esterification, with the DS diminishing only on the average from 0.18 to 0.15 in both butyration and benzoylation, respectively. The DS determination with different methods gave values in a same range. As an example, DS determined by RP-HPLC analysis and by quantitative ^{13}C NMR showed values of 0.77 and 0.72 for GGM-Bz13 and 0.25 and 0.27 for GGM-Bu8, respectively. A LiCl/DMF solvent system has been successfully used for dextran, glucan, and xylan esterification, (Heinze et al., 2006) while a LiCl/DMF solvent system with DMAP was successfully used for esterification with hemicelluloses and with guar gum with succinic anhydride (Fujioka et al., 2009; Sun et al., 2001). Hence, DMAP was trialled in benzoylation with pyridine and LiBr in butyration as an extra catalyst.

5.3.2. Benzoylation (II)

The best RE-% in benzoylation was obtained with low quantities of reagent at 100 °C or higher temperatures. RE became higher in DMF than in pyridine (GGM-Bz1 and GGM-Bz2, Table 4). GGM was not dissolved in DMF-pyridine well enough at 40-45 °C and that led to low RE-%. Results also showed that extending the reaction time from 2 to 22 h did not increase the average DS at 100 °C. The RE and DS are contradicting; the increase of quantity of reagent from 1.1 eqv. to 3.3 eqv. of reagent in the 22 h benzoylation at 100 °C increased the DS values from 0.38 and 0.77, but decreased the RE value from 35% to 23%, respectively (GGM-Bz11 and GGM-Bz13, Table 4). A temperature increment from 70 °C to 100 °C in the 1 h reaction increased the RE value from 23% to 50%, respectively (GGM-Bz4 and GGM-Bz5, Table 4). The determined molar yields were 82% or higher.

Table 4. Reaction parameters and analysis results in benzoylation. n.d. = not determined. 1) Pyridine/DMF ratio (v/v) 2:1, (1:5 with others). 2) XAD-8 purified GGM used. 3) 0.33 equiv/sugar unit of dimethylaminopyridine with pyridine.

GGM-Bz	Eqv./ unit of Benzoic anhydride	Reaction temperature [°C]	Reaction time [h]	DS of benzoic group	DS of acetyl group	RE-%	Molar mass [kg/mol]	T_g [°C]	$T_d^{10\%}$ [°C]
1	7.5[1]	40	70	0.02	n.d.	0.3	100	n.d.	n.d.
2	6.6	45	70	0.07	n.d.	1.1	86	n.d.	n.d.
4	0.3	70	1	0.07	0.16	23	76	77	n.d.
5	0.3	100	1	0.15	n.d.	50	n.d.	n.d.	n.d.
6	0.8[2]	100	1	0.11	n.d.	13	100	n.d.	n.d.
7	0.8	100	1	0.33	n.d.	41	80	n.d.	n.d.
8	0.8	100	2	0.37	n.d.	46	n.d.	85	254
9	3.3	100	5	0.64	n.d.	19	80	n.d.	n.d.
10	0.8[3]	100	22	0.36	n.d.	43	77	n.d.	n.d.
11	1.1	100	22	0.38	n.d.	35	81	n.d.	n.d.
12	2.2	100	22	0.59	n.d.	27	87	n.d.	n.d.
13	3.3	100	22	0.77	n.d.	23	72	n.d.	n.d.
14	3.3	130	1.5	0.75	0.14	23	110	n.d.	n.d.
15	3.3[3]	130	1.5	0.93	n.d.	28	120	n.d.	n.d.
16	2.2	130	5	0.78	n.d.	35	n.d.	n.d.	n.d.
17	3.3	130	5	0.92	0.15	28	n.d.	68	303
18	4.4[3]	130	22	0.82	n.d.	19	75	73	331

5.3.3. Butyration (II)

The best RE-% values were achieved with small amounts of reagent, 36% at best with 0.25 eqv. of reagent, in comparison to 19% with 1.5 eqv. of reagent at 90 °C for GGM-Bu4 and GGM-Bu9, respectively (Table 5). Butyric anhydride made a deficient solubility of GGM in DMF-pyridine, that is, heterogeneous reaction, which was compensated by elevated temperatures. A temperature increment led to increased RE-% (Table 5, GGM-Bu2 and GGM-Bu5). A catalytic amount of LiCl was added to the reaction, but it decreased the DS (GGM-Bu6 and GGM-Bu7). As the product precipitated during purification, different solvents during purifications influenced on molar yield of the products due to different solubility of the GGM esters: the yield with 1:2:7 methanol/ethyl-acetate-2-propanol for GGM-Bu8 was 94% and clearly the best, while 90% methanol for purification of GGM-Bu3 (DS = 0.30) gave a 68% yield, being the lowest yield of the tested samples. 2-Propanol as a solvent for precipitation for GGM-Bu4 (DS = 0.30) gave a yield of 86%.

Table 5. Reaction parameters and results in butyration . n.d. = not determined.

GGM-Bu	Ekv. of butyric anh. / SU	Reaction T [°C]	Reaction time [h]	Solvent in product purification	DS of butyric group	DS of acetyl group	RE-%	Molar mass [kg/mol]	T_g [°C]	$T_d^{10\%}$ [°C]
1	2.0	45	96	90% EtOH	0.02	n.d.	1.0	90	n.d.	n.d.
2	0.5	70	1.5	90% 2-propanol	0.06	n.d.	12	n.d.	79	240
3	1.5	85	3.5	90% MeOH	0.30	0.15	20	76	82	250
4	0.25	90	1.5	90% 2-propanol	0.09	n.d.	36	75	n.d.	n.d.
5	0.5	90	1.5	90% 2-propanol	0.13	0.15	26	82	n.d.	n.d.
6	0.5	90	3.5	90% 2-propanol	0.15	n.d.	30	68	n.d.	n.d.
7	0.5[1]	90	3.5	90% 2-propanol	0.13	n.d.	26	65	n.d.	n.d.
8	1	90	2	1:2:7 of MeOH:ethyl acetate:2-propanol	0.25	0.14	25	85	75	251
9	1.5	90	3.5	90% 2-propanol	0.29	n.d.	19	94	n.d.	n.d.
10	1.5	130	3.5	90% MeOH	0.50	n.d.	33	n.d.	n.d.	n.d.
11	2.0	130	3.5	90% EtOH	0.61	n.d.	31	n.d.	n.d.	n.d.
12	3.0	130	3.5	90% EtOH	0.69	n.d.	23	82	68	275

5.3.4. Phthaloylation (III)

The reactions with lowest amount of reagent yielded higher RE-% (0.5 eqv., 52-64%) than the reactions with higher amount of reagent (2 eqv., 31-32%, Table 6). The highest DS value of 0.81 was achieved with a large amount of reagent. The increased reaction temperature compensated the long reaction time. Dimethylaminopyridine was trialled as an additional catalyst, but did not have a major effect on the RE-% (GGM-Ph5).

Table 6. Reaction parameters and analysis results in phthaylation. n.d. = not determined. DMAP = dimethylaminopyridine

GGM -Ph	Eqv. of phthalic anhydride	T (˚C)	Reaction time [h]	DS HPLC	DS NMR			RE-%	GGM type
					^{1}H	^{13}C	^{13}C DS-% of C6		
1	0.27	70	2	n.d.	0.14	n.d.	n.d.	52	LMW-GGM
2	0.35	70	2	n.d.	0.19	n.d.	n.d.	55	GGM
3	0.35	70	2	n.d.	0.21	0.23	24	56	LMW-GGM
4	0.5	70	2	0.32	n.d.	0.29	36	64	HMW-GGM
5	0.5^{DMAP}	*100*	2	0.35	n.d.	n.d.	n.d.	70	HMW-GGM
6	1	100	2	0.51	n.d.	n.d.	n.d.	51	HMW-GGM
7	*2.0*	70	22	0.61	0.69	n.d.	n.d.	31	HMW-GGM
8	*2.0*	100	2	0.63	n.d.	0.71	51	32	HMW-GGM
9	5.6	100	22	0.81	n.d.	n.d.	n.d.	15	HMW-GGM

5.3.5. Succinylation of GGM (IV)

The reaction optimisation was not carried out and only LMW-GGM was used in succinilation. The synthesis aiming at two different DS values was accomplished. The DS values were 1.6 and 0.94. High DS GGM-Su was soluble in ethanol, unlike the other esters of GGM (II-IV).

5.3.6. Characterisation of the GGM esters (II-IV)

We aim at describing the chemical character of the modified biopolymer GGM. Solubility determinations reveal the nature of interactions with solvents. Moreover, the molar mass can be determined in combination of SEC and laser light scattering and RI detectance. Upon determining the quantity of the desired functional group with two or more different analytical techniques, there ought not to appear any ambiguities but rather supplementary information of the chemical physical character of the GGM derivative in relation to unmodified GGM. However, there may be some minor differences in the quantitative results, hinting that no method can reveal the absolute truth, but rather render the close approximate of it.

The degree of substitution was studied with ^{13}C NMR, RP-HPLC, and ^{1}H NMR. MALDI-TOF-MS supports the NMR by showing covalent bonding of the substituents. The benzoyl, butyryl, and phthaloyl contents of the GGM esters were determined by hydrolysing the ester groups with alkali and analysing the corresponding acid of the modified GGMs by RP-HPLC. The DS values of phthalaylation obtained with the quantitative ^{13}C NMR, ^{1}H NMR, and HPLC methods were approximately at the same range and thus the results were independent of the choice of analysis method.

5.3.7. Thermal properties of the GGM esters (II)

The acetylated GGM had a trend of increased $T_d^{50\%}$ at an increased degree of acetylation (Tables 4-5). On the other hand, highly succinylated hemicelluloses have been shown to have a lower $T_d^{50\%}$ value than the native hemicelluloses (Peng et al, 2012). In our study, there was a general trend of an increase in $T_d^{10\%}$ of the butyric or benzoic esters upon an increase in DS, with a clear exception for GGM-Bz18 with the high $T_d^{10\%}$ value of 331 °C. GGM-Bz18 was prepared with DMAP, which may have had an impact on the regional substitution pattern (Dicke, 2004) and consequently on the T_d value. However, the starting GGM had a $T_d^{10\%}$ value of 262 °C, which is higher than those of GGM-Bz and GGM-Bu with DS values of 0.37 and 0.30 respectively. T_g determined with DSC was lower with esterified GGM than the 86 °C for EtOH precipitated native GGM. There was no clear trend observed in T_g correlating with the DS, though the GGM esters with high DS had the lowest T_g values.

5.3.8. MALDI-TOF-MS (III)

GGM-Ph was analysed using oligosaccharide fingerprinting after enzymatic treatment and combined with MALDI-TOF-MS (see chapter 5.2.5). The main products of the enzymatic hydrolysis were assigned to the GGM oligomers with phthalic groups with an m/z increment of 142, and acetyl groups with an m/z increment of 42 (Figure 16). The fractionation pattern fitted well with DS^{Ph} 0.19 and DS^{Ac} of 0.21. Oligomers with 2-5 sugar units had either acetyl groups or phthalate groups, or both of them. This refers to some extent to a heterogeneous regional reaction pattern.

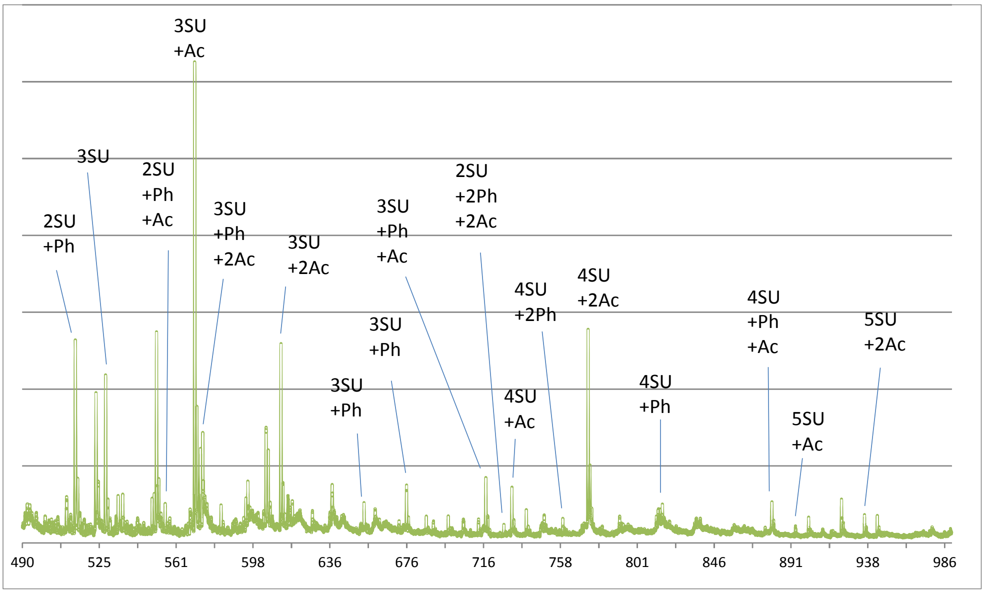

Figure 16. MALDI-TOF-MS of GGM-Ph2 with a DS value of 0.19. GGM-Ph was enzymatically hydrolysed to its oligomers prior to analysis. SU = sugar unit, Ph = phthalic group, Ac = acetyl group.

5.3.9. NMR (II-IV)

With quantitative ^{13}C NMR the degree of substitution was quantified by the ratio of the signals of the substituents (benzoyl, butyric, phthaloyl and succinyl) to the signal of anomeric carbon, taking into account of the number of carbons in a substituent (Figures 17-20). The quantitative ^{13}C NMR spectrum of GGM was used as a reference (Figure 9). The appearance of correct signals in NMR is a proof of covalent bonding alongside with the other analysis. There are some challenges concerning the regional substitution patterns because of the hetero character of the GGM backbone (discussed in a chapter 5.2.6., Figure 9) Since acetyl groups remained untackled in the esterification, quantifying GGM-Ph and GGM-Bz with ^{1}H NMR was based on the known DS of acetyl groups according to the quantitative ^{13}C NMR (III). The carbonyl carbons of acetyl and the introduced ester groups can be distinguished with Heteronuclear multiple-bond correlation spectroscopy (HMBC, II) The ratio of DS between C6 and C2+C3 can be determined with quantitative ^{13}C NMR by measuring the decrease of the non-substituted C6 signal of the GGM ester in comparison to the non-substituted C6 signal of native GGM. The C6 signal at δ = 59.0-62.0 ppm of non-substituted C6 decreases in size and shifts to around 63-68 ppm, partially overlapping with the signals of C2 and C3 (Ekholm et al., 2012; Hannuksela and Hervé du Penhoat, 2004). A complimentary way to determine DS is by integrating the carbonyl groups of the phthalic or succinic group and then the DS value can be obtained by the subtraction of the value of the carbonyl signal of the acetyl group from the value of the entire carbonyl range (III-IV). This determination confirmed the DS values, since the results were in the same range as with the other methods.

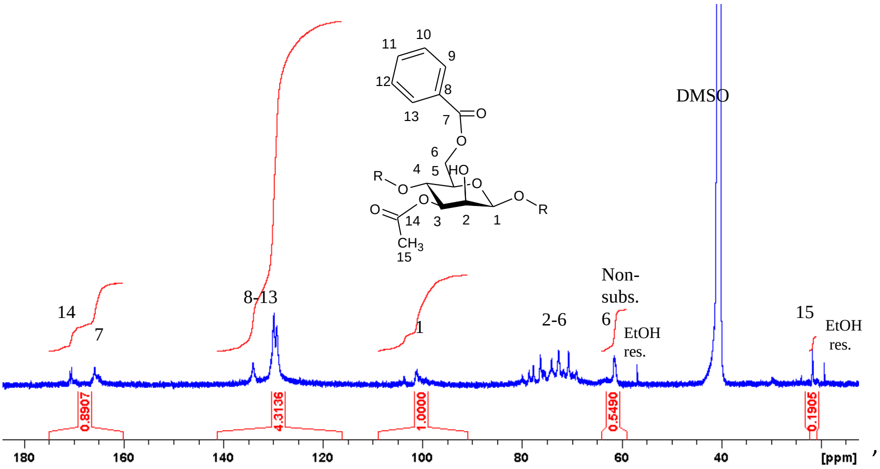

Figure 17. Quantitative ^{13}C NMR of GGM-Bz13.

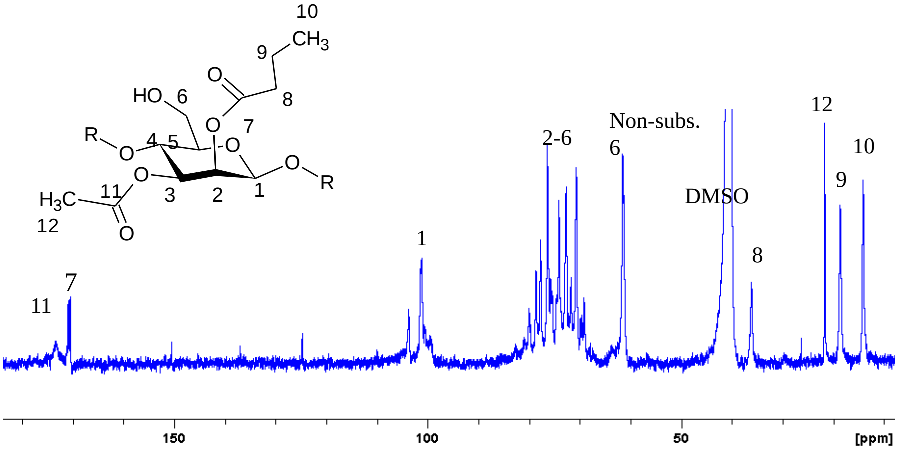

Figure 18. Quantitative ^{13}C NMR of GGM-Bu8.

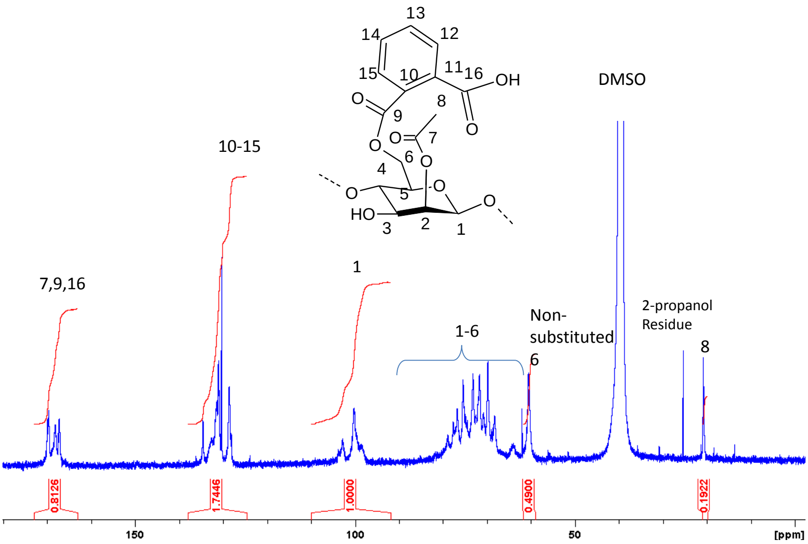

Figure 19. Quantitative spectrum of ^{13}C NMR of GGM-Ph4.

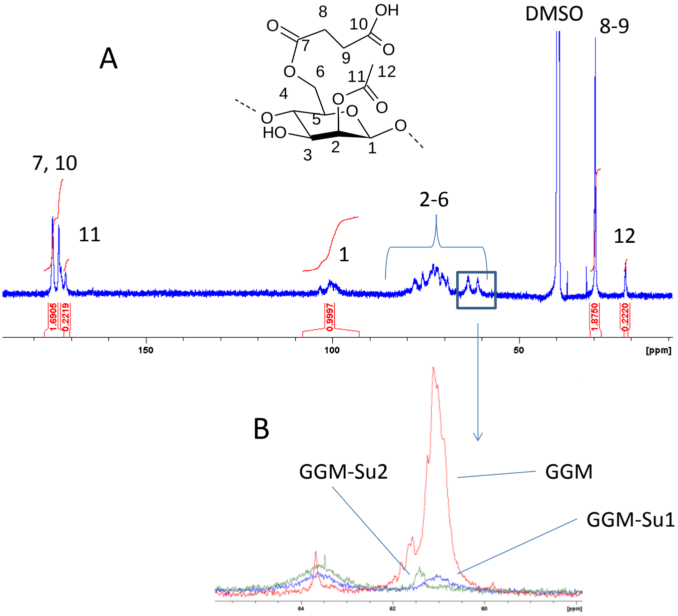

Figure 20. Quantitative ^{13}C NMR spectrum of GGM-Su1 (A). C6 substitution pattern of the GGM and GGM-Su1 and GGM-Su2 with the quantitative C^{13} NMR (B). The signal of non-substituted C6 is at δ = 60-62 ppm, while the signals of GGM-Su1 and GGM-Su2 has shifted to δ = 63-66 ppm.

5.3.10. Molar mass (II)

Molar mass measurements were carried out by SEC combined with MALLS-RI detectors. 0.05 M LiBr DMSO was used as the eluent. The GGM esters did not dissolve adequately in water, whereas polar and aprotic DMSO dissolved well both GGM and GGM esters with varying degrees of hydrophobicity. However, especially native GGM and low substituted samples may contain molecular aggregates or dispersed micro-particles in DMSO, which significantly influenced the measurements by the MALLS/RI system. A polyelectrolyte effect is caused by the local charges along the polysaccharide due to possible acidic residues in GGM. LiBr was added to the eluent to prevent the polyelectrolyte effects and avoid artificial peaks in the chromatograms. The essential d*n*/d*c* value was determined for the GGM-Bz7 (DS 0.33) in 0.05 LiBr DMSO solutions. The obtained value 0.073 was used for GGM and GGM esters in this solvent. Figure 21 A-C demonstrates a SEC-MALLS/RI chromatogram of the GGM-Bz14 (DS 0.75) containing mostly dissolved polymers, giving more accurate determination of molar mass characteristics. The ‘entire size distribution’ in Figure 21 A includes molecular aggregates and dissolved polymers. The ‘dissolved polymers’ in Figure 21 B exclude the molecular aggregates. The ‘partial size distribution’ of dissolved polymers in Figure 21 C elucidates the distribution of dissolved polymers without aggregates and the largest polymers. The results are shown in Table 7. The higher the DS of the GGM ester, the less aggregate formation and the narrower was the polydispersity (M_w/M_n). In general, the higher the degree of substitution, the higher was the average molar mass (Tables 4-6). In addition to that, there is a general trend of slightly reducing molar mass with an increasing reaction time.

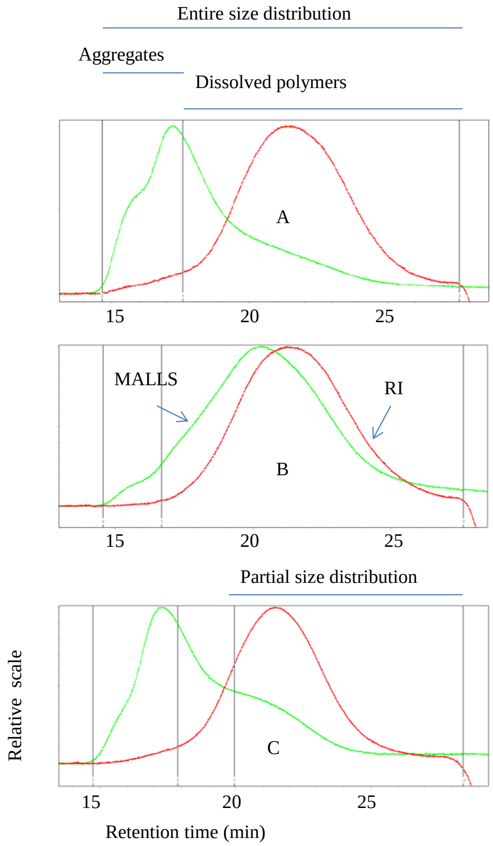

Figure 21. SEC-MALLS chromatograms of ethanol precipitated native GGM (A), GGMBz14 (B, DS 0.75), and GGM-Bu5 (C, DS 0.13) in 0.05 M LiBr DMSO. When RI and MALLS curve patterns are following each other, the sample is mostly dissolved. In the Figure A there is probable aggregation of GGM. In the Figure B there are mostly dissolved polymers giving more likely the accurate molar mass of GGM-Bz14. In the Figure C there is also aggregation to some extent of GGM-Bu5, the partial size distribution excluding aggregates and the largest polymers.

Table 7. The molar masses of GGM, GGM-Bz and GGM-Bu; the entire size distribution includes aggregates and dissolved polymers, dissolved polymers exclude aggregates and partial size distribution excludes molecular aggregates and the largest polymers in SEC-MALLS analysis

	DS of butyryl or benzoyl group	Aggregates M_w [kg/mol] / M_w/M_n	Dissolved polymers M_w [kg/mol] / M_w/M_n]	Entire size distribution M_w [kg/mol] / M_w/M_n	Partial size distribution
GGM	-	1250/1.1	52/1.6	96/2.9	n.d.
GGM-Bz14	0.75	1140 / 1.1	102/1.2	108/1.2	n.d.
GGM-Bu5	0.13	1190 / 1.0	56/1.7	82/2.5	28/1.1

5.3.11. Solubility (II-IV)

The solubility in water or lack of it is an issue in industrial and laboratory-scale applications; water as solvent is appreciated for its non-toxicity and low cost. Some organic solvents may have toxicological effects and may require specific processing circumstances and would thus render a controversial image of otherwise sustainable biopolymeric applications. However, organic solvents provide an effective way to derivatise hemicellulos as aiming at hydrophobic nature. The solubility is depending for instance on the chain length, DS, and the polarity of the substituent. The solubility of GGM esters is illustrated in Table 8. The lower the non-polar substitution, the higher is the water solubility. The higher the DS, the higher becomes the possibility for being soluble to organic solvents like DMF, DMSO, or ethanol. Benzoic and butyric groups are non-polar and the DS value of 0.37 makes them hydrophobic. GGM-Bu and GGM-Bz were only partially water soluble with low DS values of 0.07 and 0.13. The succinic and phthalic substituents have got a carboxyl group, affecting the solubility in polar direction too. GGM-Ph is 55% water-soluble with the DS value of 0.51. The chain length of LMW-GGM-based and GGM-Ph2 and GGM-based GGM-Ph3 made a slight difference.

Short chain length makes biopolymers more mobile; the high DS (1.6) of LMW-based GGM-Su2 was soluble in 67% (v/v) of ethanol-water and in protic ethanol but not in water, while low DS (0.94) GGM-Su1 was soluble in water. In comparison, GGM-Ph5 with DS 0.51 was only 55% soluble in water. Preparing GGM-Ph, GGM-Bz, and GGM-Su with optimised DS we obtained slight hydrophobicity but maintained the dispersability in water (III-IV). GGM-Bu and GGM-Bz with the DS value of 0.75 was soluble in aprotic DMF and partially soluble in aprotic DMSO at ambient temperature, while GGM-Bu and GGM-Bz with DS 0.07-0.37 were insoluble in these solvents. However, heating the GGM and its derivatives to 50 °C in DMF or DMSO did solubilise GGM and its esters regardless of DS or molar mass.

Table 8. Solubility of GGM esters in water and ethanol. 1) LMW-GGM, otherwise GGM n.d. = not determined. s. = soluble, i.s. = insoluble.

	GGM-Bu5	**GGM-Bu8**	**GGM-Bz4**	**GGM-Bz8**	**GGM-Bz14**	**GGM-Ph2[1]**	**GGM-Ph3**	**GGM-Ph6**	**GGM-Su1[1]**	**GGM-Su2[1]**
DS	0.13	0.25	0.07	0.37	0.70	0.20	0.19	0.51	1.0	1.6
Water [wt-%]	68	63	77	13	5	97	91	55	s.	i.s.
Ethanol [wt-%]	n.d.	n.d.	n.d.	n.d.	n.d.	19	20	30	i.s.	s.

5.4. Applications (III-IV)

5.4.1. The barrier functionality (III-IV)

Polysaccharides can make excellent oxygen barriers due to an extensive network of hydrogen bonding and good grease barriers due to intrinsic polarity and consequent resistance to non-polar fats. In this work we made GGM polymers less polar, but still tried to maintain or even improve the grease barrier properties. The structure-property relationship was thus studied to find out if GGM esters incorporated in or onto NFC or onto cartonboard may have higher barrier properties than the pure substrate. The chemical structure-property relationship of GGM-Su, GGM-Bz, or GGM-Ph was examined as coating on cartonboard with an inorganic pre-layer and on NFC-GGM composites by oxygen, water, grease barrier, and mechanical (dynamic mechanical analysis) testing.

A polysaccharide-based packaging is usually too water sensitive for any occasional moisture. In order to make the coatings or composite films hydrophobic, the polarity of the GGM has to be reduced (Cunha and Gandini, 2010; Hartman et al., 2006). This was here done by introducing non-polar hydrocarbon moieties, where the esterification of GGM rendered the means to decrease the hydrophilicity of GGM in a controlled manner. To be able to use water in coating applications, GGM was esterified to low DS so that it was still dispersible in water.

Coating on a substrate saves the material by having the appropriate functionality only on the surface, which is exposed to the appliance. The functionality in this case was the GGM ester upon being the enhancer of the barrier properties. We utilized the natural oleophobic nature of polysaccharides as grease barriers (Kjellgren et al., 2006). When surface coating is chemically distinct from the substrate matrix, inadequate substrate/coating compatibility may occur. In this perspective, the use of a GGM derivative is advantageous because the affinity between NFC and GGM is good (Eronen et al., 2011). NFC is known for its high mechanical strength (Isogai, 2013), while hemicelluloses are known for their good barrier properties (Kochumalayil et al., 2013). In this study, the mechanical strength is possessed by a cartonboard matrix or a NFC network. GGM-Ph and GGM-Bz with low DS exhibited features toward hydrophobicity but were still dispersible in water in processing. Not being water-soluble, GGM-Su with DS of 1.6 was dispersed in ethanol.

5.4.2. GGM esters as barrier coatings on cartonboard (III)

Overview

Grease resistance is essential for food packaging, where the food item includes fats. The packaging ought to resist grease a few minutes or several days depending on the use. GGM-Bz and GGM-Ph with DS 0.16-0.21 and GGM were utilised as barrier coatings against water and grease on cartonboard with an inorganic pre-layer. The SEM images showed a layer of GGM or GGM esters on a fairly rough inorganic layer of a cartonboard, which is almost penetrating the thin 1.2 g/m^2 GGM-Ph coating (Figure 22). Also the thickness of the coating varied on the rough surface. However, there was no visible evidence of pinholes of the coatings. Grease resistance against rapeseed oil was determined with the applied method of ASTM, while WVTR was determined for water vapour resistance.

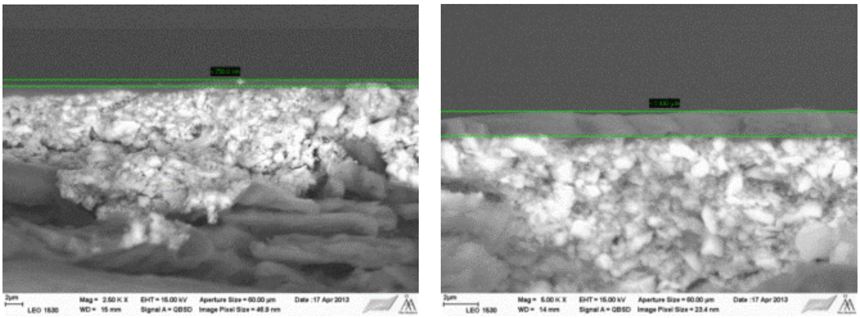

Figure 22. Pre-coated cartonboard coated with GGM-Ph (1.2 g/m^2, left) and GGM-Bz15 (2.6 g/m^2).

Water vapour and grease barrier

A practical method for obtaining the active barrier lifetime against oil is a prism method (Bollström et al., 2012). The penetration of grease through the substrate is monitored as a function of time as changes in the refractive index at the prism-cartonboard interface (III) at ambient temperature and 22-30 % R.H. The degree of penetration is quantified with image analysis (pixel count) as a function of time. The threshold value was set to 0.1% penetration. The results are described in Table 9 and in Figure 23. The measurements were carried out in ambient conditions for 1-3 g/m^2 coatings. The coloured oil was absorbed onto the paperboard upon the penetration of the coated cartonboard. GGM-Bz and GGM-Ph (GGM-Ph3) double coating, 2.4 g/m^2, resulted in 47 h and 54 h resistance, while the non-coated cartonboard had only 0.7 h resistance. High-molar-mass-based GGM gave advantage over the low-molar-mass GGM; HMW-GGM-Ph gave almost three-fold longer grease resistance than GGM-Ph. GGM-Bz yielded better grease resistance than GGM-Ph with single 1.2 g/m^2 coating. An additional coating by another layer significantly increased the barrier properties from 10 to 54 h of GGM-Ph and also gave the advantage over the GGM-Bz. The plausible cause for this is the compensating cover of the uncovered micro areas of the single coating. The inorganic pre-layer of cartonboard was not entirely compatible with the organic coatings. With thick ~10 g/m^2 coatings we used the ASTM F119-82 method where there is an external pressure on the sample. The threshold was three penetrated samples out of the six. GGM-Ph and GGM-Bz with thickness of ~10 g/m^2 coatings gave 74 h and 51 h olive oil resistance, respectively.

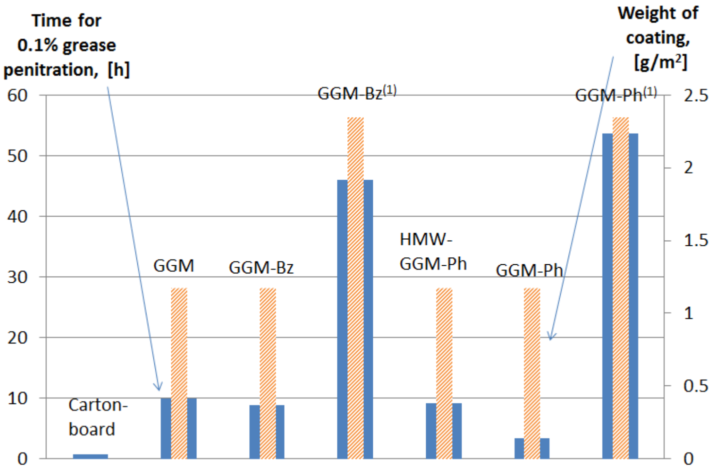

Figure 23. Grease barrier penetration of cartonboard coated with GGM, GGM-Bz (DS 0.16), GGM-Ph (GGM-Ph3, DS = 0.21) or HMW-GGM-Ph (GGM-Ph2, DS = 0.19) determined at ambient temperature and at 22-30% R.H. (1) = two coating layers instead of one layer. HMW-GGM-Ph is based on GGM; others are based on LMW-GGM.

Water vapour transmission values were determined and compared to a blank reference as %-values in Table 9 and the results are illustrated in Figure 24. The ester groups of GGM clearly decreased the hydrophilicity. WVTR was lower for the GGM esters than for GGM. Obviously, the thicker the coating, the lower the WVTR values were. Surprisingly, triple GGM-Bz coating (3.5 g/m^2) gave lower water vapour resistance than single coated (2.6 g/m^2) cartonboard. GGM-Ph rendered stronger barrier with thick coating (~10 g/m^2) than GGM-Bz with 39 and 85 g/m^2/24 h, respectively. On the contrary, GGM-Ph had lower ability to hold water with thin coating (1.2 g/m^2) than GGM and GGM-Bz. This may be due to some patchiness in the coating due to lack of adherence of the thin-coated GGM-Ph layer with the inorganic layer of the cartonboard. The molar mass of GGM and GGM-Ph made a difference: HMW-GGM and HMW-GGM-Ph gave better water vapour barrier than LMW-based GGM and GGM-Ph. The lowest absolute value was 39 g/m^2/24 h with HMW-GGM-based GGM-

Ph. GGM-Ph contains carboxylic groups, unlike GGM-Bz, which decreased the hydrophobicity. GGM-Ph had higher DS (0.21 versus 0.16) than GGM-Bz though and this in turn increased the hydrophobicity. The low DS GGM coatings could be used for packaging requiring occasional water vapour resistance.

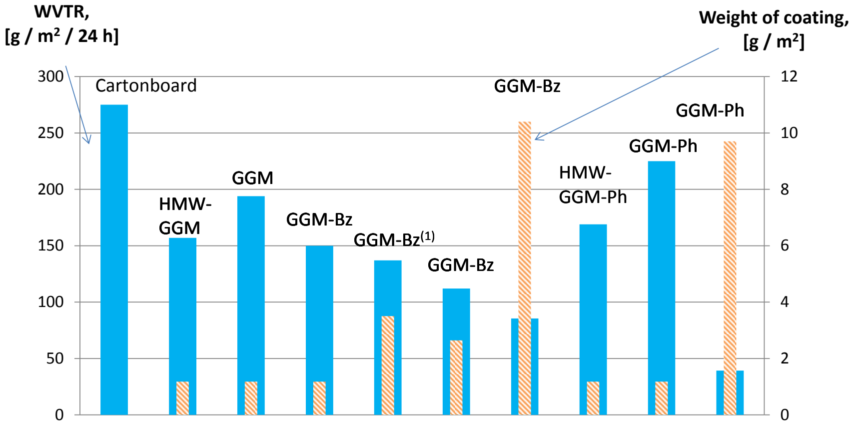

Figure 24. Water barrier penetration of pre-coated cardboard with GGM, GGM-Bz or GGM-Ph coating. (1) = Triple coating, otherwise single coating. HMW-GGM-Ph is based on GGM; others are based on LMW-GGM.

Table 9. The results of WVTR at 23 °C at 50 % R.H. and grease penetration.

The coating on a Cartonboard	Weight of the coating layer [g/m^2]	Number of coating layers	WVTR [g/m^2/ 24 h]	% of WVTR decrease in comparison to plain cartonboard	Time of rape seed oil barrier 0.1% of penetration [h]	Olive oil penetration 3 of 6 samples [h]
	-	-	278	-	0.7	n.d.
GGM	1.2	1	194	29	9.7	n.d.
HMW-GGM	1.2	1	157	43	n.d.	n.d.
GGM-Bz	3.5	3	137	50	n.d.	n.d.
GGM-Bz	2.4	2	n.d.	n.d.	47	n.d.
GGM-Bz	2.6	1	112	59	n.d.	n.d.
GGM-Bz	1.2	1	150	45	10.4	n.d.
GGM-Bz	10.4	1	85	69	n.d.	51
GGM-Ph	2.4	2	N.d.	-	54	n.d.
GGM-Ph	9.7	1	39	86	n.d.	74
HMW-GGM-Ph	1.2	1	169	39	9.1	n.d.
GGM-Ph	1.2	1	225	18	3.4	n.d.

5.4.3. Composite films of nanofibrillated cellulose and GGM coated with succinic esters of GGM (IV)

Introduction

Food packaging requires that the material withstand alterations in humidity. We approached this by determining stiffness as a function of R.H. Stiffness is good for packaging, which does not require flexibility (Mittal, 2011). Nanofibrillated cellulose - GGM composite films were coated either with a novel succinic ester of GGM or with native GGM. NFC films were made as reference (Figure 25). The succinic ester of GGM was synthesised at low (GGM-Su1) and high (GGM-Su2) degree of substitution to obtain different level of hydrophobicity. GGM and its succinic esters had good affinity to the NFC substrate. This made it possible to implement the barrier functionality on the NFC network with adequate mechanical properties. Hemicelluloses are known to have excellent oxygen barrier properties (Escalante et al., 2012) and NFC is known to have excellent mechanical properties (Isogai, 2013). The fibrils of NFC have been described as being of small diameter and high aspect ratio and possessing high strength (Pahimanolis et al., 2013). We targeted to mimic the plant cell wall structure of hemicellulose, cellulose and lignin by making a composite with robust web like structure of NFC and GGM and GGM-Su (Stevanic et al., 2014). GGM can also be considered to function as nano-size filler in a NFC network, but connected to NFC by hydrogen bonding. Hence, even with the added hydrophobic functionality, GGM can be well-integrated in the NFC network due to their chemical similarities. We aimed to enhance the grease- and oxygen barrier properties with GGM and GGM-Su coatings and the hydrophobicity with GGM-Su coatings and with GGM in the NFC network.

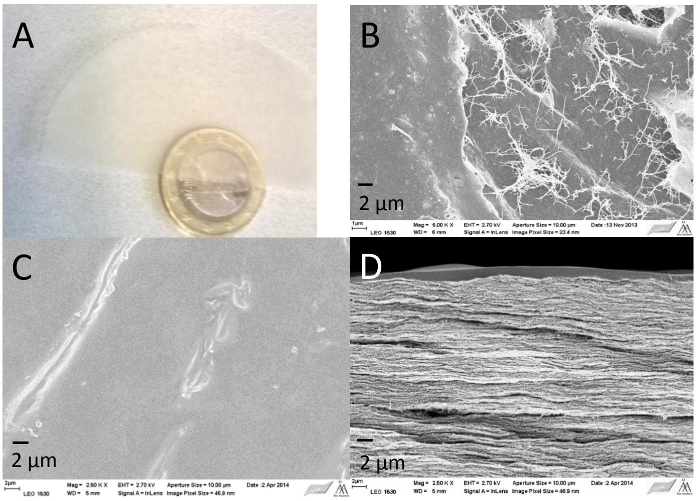

Figure 25. Photo of translucent NFC-GGM film (A), and SEM pictures of the NFC-GGM film (B), NFC-GGM film coated with GGM-Su1: a top (C) and of a cross-section (D) image.

The amount of GGM in the NFC films was optimised by absorption tests, resulting in 5.5 wt-% of GGM in the film. The amount was in line with the mechanical properties. The coating resulted in 5.4 wt-% increase on a film, yielding translucent films (Figure 25). The GGM-Su1, GGM-Su2 and GGM were applied on the NFC-GGM film and GGM-Su2 also on the NFC film. Ethanol was used as solvent for the coating GGM-Su2 (high DS), while water was used for the rest. Based on our previous studies, 15 wt-% of sorbitol (relative to GGM) was added to the dispersions to give more coherent film-like structure and potentially better oxygen barrier properties.

Water interaction with the film surface

We observed the wetting behaviour of the film surface with the sessile water drop CA determination method. Surfaces showing water CA > 90° lean towards hydrophobic behaviour and CA < 90° lean towards hydrophilic behaviour. The Young equation describes the wetting on ideal surfaces and does not consider the impact of surface topography. However, when water drop volume and baseline (wetting diameter of the drop) information is used side-by-side with the CA, additional information about film heterogeneity or water absorption into the film can be unveiled. The representative individual cases are illustrated in Figures 26 and 27 and the average CA value at 1 second are given in Table 10.

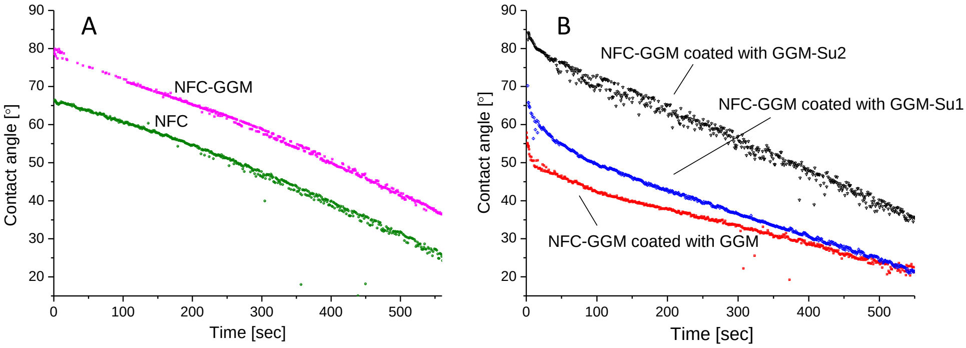

Figure 26. The water contact angle values as a function of time on NFC-GGM and NFC films (A) and NFC-GGM films coated with GGM-Su2, GGM-Su1 and GGM (B).

Table 10. The water contact angle value on the films at 1 second.

The matrix	The coating	Water CA at 1 s [°]
NFC	-	63±3
NFC	GGM-Su2	67±6
NFC-GGM	-	76±6
NFC-GGM	GGM	55±1
NFC-GGM	GGM-Su1	61±6
NFC-GGM	GGM-Su2	78±5

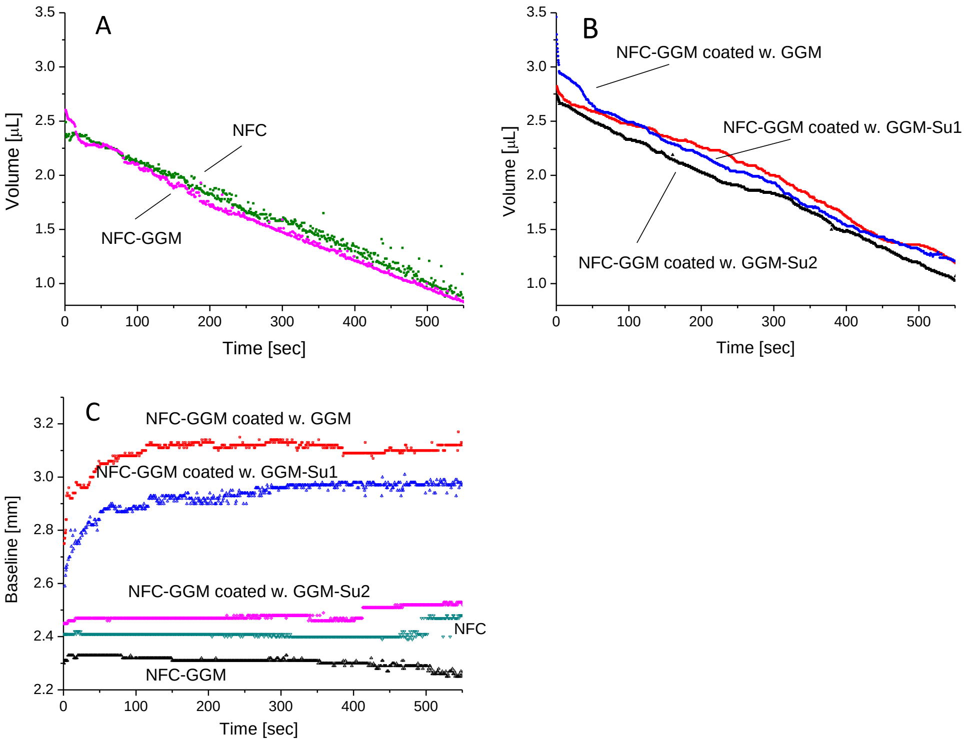

Figure 27. The water drop volume (A and B) and baseline (C) as a function of time on a film surface.

Our results can be split into two categories based on the film wetting properties. In the first category, films produced solid, sloped straight line CA and drop volumes complemented with flat baselines as a function of time. The baseline remained fairly constant, i.e. there was no increase of the wetting area throughout the measurement. Hence, the change in CA over time was solely dependent on the evaporation of the drop. The pristine NFC and NFC-GGM films and NFC-GGM film coated with GGM-Su2 belong to this category. The NFC-GGM film coated with GGM-Su2 showed the highest CA (78°) of the three. Hydrophobic domains on the surface hinder water molecules from advancing. Surprisingly GGM within the NFC film increased the CA in comparison to the pristine NFC film. Spiridon et al (2013) suggested that addition of cellulose into starch-based composite films improves their water resistance due to strengthened inter-component hydrogen bonding (Spiridon et al., 2013). The extensive hydrogen bonding between GGM and NFC may disfavour the hydrogen bonding sites for water molecules (Kwak et al., 2001). Acetyl groups makes GGM water-soluble for spacing out the polymer chain, but upon incorporated onto the solid film matrix, they increased the hydrophobicity.

In the second category for NFC-GGM coated with GGM or GGM-Su1 it took roughly 100 seconds for the CA curve to straighten up. The baseline graph shows similar delayed increase of the wetting area.

Both these films have lower initial CA than the pristine NFC film or NFC-GGM composite film (Table 10), making them more hydrophilic than their counterparts in the first category. The advancement of the CA went hand-in-hand with the non-linear increase of the baseline, which kept the drop volume constant over time – an indication of non-absorption of water into the film matrix.

The grease barrier properties

Grease barrier was determined with the method where a cylinder on top of the film was filled with surplus of coloured rapeseed oil. With this method there was no extra pressure enforced onto the grease on the biofilm. Biopolymer films have the tendency of poorer barrier and mechanical properties at elevated R.H. We tested the grease barrier for rapeseed oil in exotic conditions, where the edges of the film were exposed to the high R.H. No oil penetration was observed for NFC-GGM at 60 °C and at 75% R.H. in five-day-long tests. Both the pristine NFC films and the NFC-GGM composite films coated with NFC-GGM-Su1 were also impenetrable at 50 °C and at 50% R.H. in six-day-long tests. NFC-GGM composite film coated with GGM-Su2 was impermeable for 11 days at 50 °C and at 40% R.H. followed by ten months at 23 °C at 50% R.H. The SEM pictures show the possible oil deposition on a surface of the film (Figure 28).

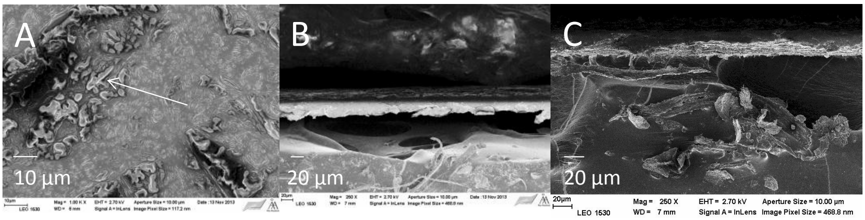

Figure 28. SEM pictures of the possible oil deposition on a surface of NFC-film after 6 days exposure at 50 °C and at 50% R.H. as picture (A) and as a cross-section, where the surface has turned to dark (B), and a cross-section without the oil exposure (C).

The oxygen barrier properties

The property of oxygen permeation is crucial for biomaterials in food packaging. The lack of oxygen in a packaging reduces or diminishes the function of microbes in the food. The OP and OTR were determined from two replicates at 23 °C and at 50% R.H. and the values are shown in Table 11. GGM coating and GGM-Su2 double-coating decreased the OTR value of NFC-GGM film from 3.2 to 1.1 and 0.2 $cm^3/(m^2·d)$ respectively. The partial pressure and the film thickness differences were considered in the OP test, unlike in the OTR test. The differences were larger with OTR values than with OP values, but the trends had a resemblance. The NFC film had an OP value of 0.5 $[(cm^3·µm)(m^2·kPa·d)]$ and NFC-GGM of 0.9 $[(cm^3·µm)(m^2·kPa·d)]$. Integration of GGM made may have led to a less dense

NFC-reinforced web. GGM coating was more effective than GGM-Su1 or GGM-Su2 coatings (IV). GGM may have had better affinity onto NFC-GGM than GGM-Su and hence made a stronger barrier. However, the double-coating with GGM-Su2 gave the highest oxygen barrier with the excellent value of 0.1 [(cm^3·µm)(m^2·kPa·d)] but the standard deviation was high, 0.2. Hydrogen bonding and Van der Waals forces of the films have been that strong, that the movement of fibrils are hindered and consequently preventing oxygen permeation (Österberg et al., 2013). Thus with the modest 5.4 or 10.8 % weight increase of the film by the coating, a major enhancement in oxygen barrier properties can be achieved.

Table 11. Oxygen permeability and oxygen transmission values of the films.

Film substrate	Coating	Film thickness	OP		OTR	
		[µm]	[(cm^3·µm)(m^2·kPa·d)]	Sd	[cm^3/(m^2·d)]	Sd
NFC	-	35.5	0.5	0.07	1.4	0.2
NFC	GGM-Su2	32.5	0.3	0.00	0.9	0.03
NFC-GGM	-	28.0	0.9	0.04	3.2	0.2
NFC-GGM	GGM	35.5	0.4	0.03	1.1	0.1
NFC-GGM	GGM-Su1	37.5	0.8	0.01	2.1	0.2
NFC-GGM	GGM-Su2	43.4	0.6	0.04	1.4	0.08
NFC-GGM	GGM-Su2 X 2	49.5	0.1	0.2	0.2	0.3

To compare the OP values of other bio-based polymer films to the ones of our study, few cases are showed in Table 1 in Chapter 3.3.4. In this context, GGM-Su2 coated NFC-GGM has very competitive values, especially considering the high values of PHA and PLA.

Stiffness properties

The storage moduli of NFC and the composite films after 300 min equilibration at 0 %, 50 %, 90 %, and back to 0 % R.H. are presented in Figure 29. The storage moduli of the pristine NFC films and NFC-GGM films coated with GGM and GGM-Su2 exhibit fairly large standard deviations at 0 % and 50 % R.H., suggesting heterogeneous films with coatings. However, the average storage modulus values indicate trend-like differences between the films. All films displayed similar response with changing humidity levels; the highest moduli were observed after initial and final equilibration at 0% R.H. When the humidity was increased to 50% R.H., the moduli dropped slightly. Increasing the R.H. further to 90% led to a major decrease in moduli. The decline of storage moduli with increasing humidity is taking place because water molecules diffuse into the film structure and disturbed the hydrogen bonding within and between the NFC fibrils and GGM. As a result, GGM chains are softened, hydrogen bonding between NFC fibrils weakened, and films plasticized. When the humidity was reduced back to 0% R.H., the moduli increased sharply, exhibiting recovery between 92 and

103% relative to initial value at 0% R.H. The low moduli at high humidity and good recovery suggest slight irreversible slippage between the polymer chains and NFC fibrils within the films during exposure to humid conditions. However, the slippage is only partial and the interaction between the NFC network and the GGM preserves the film integrity well up to 50% R.H. The NFC-GGM with GGM-Su2 coating had clearly the highest recovery from 90% back to 0% R.H, addressing the adhesion between GGM-Su2 and NFC.

The addition of GGM to NFC, as a coating of GGM-Su2 on NFC-GGM films, resulted in similar stiffer films. The stiffness followed a trend-like pattern at each humidity level and remained also at 90% R.H. We attribute the higher stiffness to GGM in the NFC-GGM films, since GGM readily adsorbs on cellulose fibrils in a rigid conformation (Eronen et al., 2011). Also high debranching of galactose contributed to higher sorption of GGM to NFC (Stevanic et al., 2014). At relatively small amount (5.5 wt-%), most of the GGM can adsorb directly on NFC fibrils without ruining the hydrogen-bonded network structure. At higher concentrations, GGM and other hemicelluloses are expected to reduce the stiffness of NFC films (Hansen and Plackett, 2008). Adsorbed on NFC fibrils, GGM can potentially act as cross-linker for the NFC fibrils through hydrogen bonding, thus increasing the stiffness of NFC-GGM. GGM-Su2 on a film surface can potentially enhance stiffness via hydrogen bonding and Van der Waals forces. GGM-Su2 was more hydrophobic than GGM-Su1 and GGM and hence contributed towards the higher stiffness on a film surface in moist conditions. Water possibly disrupts the hydrogen-bonding network during coating; this may also favour stiffness of the GGM-Su2 coating where ethanol was used as solvent.

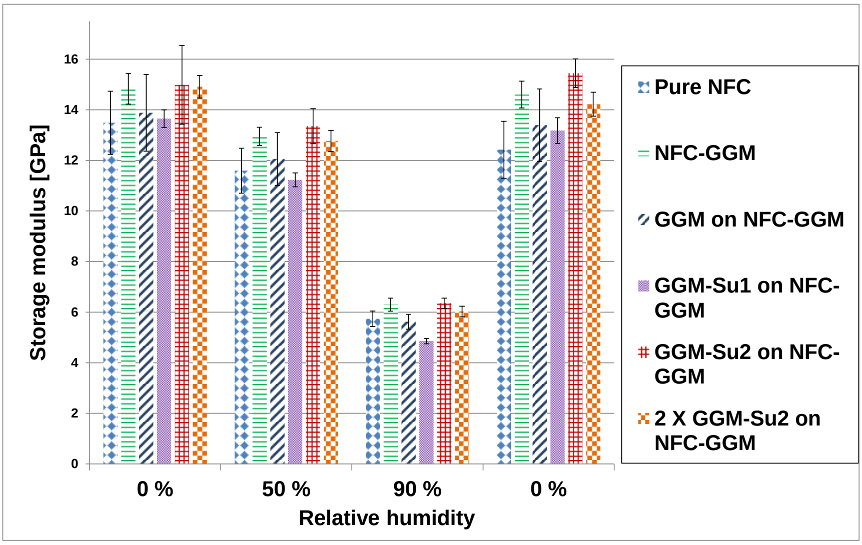

Figure 29. The storage modulus with changing R.H. of NFC, NFC-GGM, NFC-GGM coated with either GGM, GGM-Su1, GGM-Su2 or double coated with GGM-Su2.

6. Conclusions

Chemical esterification of GGM can be performed in order to enhance the barrier properties for food packaging applications. The level of hydrophobicity benzoic, butyric, phthalic, and succinic esters of GGM depend on the ester type, the DS, and the M_w of GGM. It is important to be able to determine the success of a chemical treatment through analysis. Different analytical methods such as NMR and RP-HPLC show congruence in DS determination for GGM esters and can thus be used. Polyelectrolyte titration is a well-functioning and rapid method to determine the DS for a series of cationised GGM samples along with the “slower” methods of elemental analysis and quantitative ^{13}C NMR. THF or DMSO with water enhances the RE and decreases the M_w reduction in comparison to plain water as a reaction media. With the obtained data for esterification and cationic etherification, economical methods to synthesise GGM derivatives with desired properties can be accomplished. For instance, a sensible way to alter GGM hydrophobic is the GGM benzoylation with 0.8 equivalents of benzoic anhydride reagent, where a two-hour reaction at 100 ^{o}C results in benzoic ester of GGM with the DS value of 0.37, being insoluble in water.

A major contribution to the grease barrier and a clear increase in water vapour resistance can be accomplished with thin (1-3 g/m^2) coating of GGM, GGM-Bz, or GGM-Ph on cartonboard with an inorganic pre-layer. The grease and water vapour barrier properties of the high-molar-mass-based GGM coating rise above the barrier attributes of the low molar mass-based GGM coatings. The added non-polar groups to GGM will not decrease, but rather slightly even increase the grease resistance. With this method it may be possible to replace oil-derived polymeric coatings in food packaging in terms of grease resistance. GGM esters have low DS and are thus dispersible or soluble to water, which renders this approach industrially compelling.

NFC-GGM composite films exhibit impenetrable grease barrier properties also at elevated temperatures. GGM-Su coating on GGM-NFC film and the presence of GGM within the NFC network increases the storage modulus at a wide range of relative humidity and surface hydrophobicity of the film. This is due to bridging by hydrogen bonding of the GGM-NFC network, as well as to the hydrophobic nature of GGM-Su. Double coating of GGM-Su results in really low oxygen permeability values. The level of hydrophobicity, oxygen barrier, and stiffness of the films can be adjusted by the DS value of the succinic moiety, by the thickness of the coating, and by the architecture of the composites.

7. Future prospects

Highly hydrophobic GGM esters can be studied further as functional polymers in biocomposites. Non-healthy solvents can be avoided for instance by high temperature processes. Further research ought to be carried out with multi-layer coatings of hemicellulose derivatives with bio-based polymers and/or biodegradable polymers in order to achieve adequate mechanical properties combined with the desired barrier properties for food packaging. Pilot scale experiments can be implemented with GGM-based coatings on cartonboard without inorganic pre-layering, to obtain proof of concept of the usability. The cationic GGM could possibly be applied in the following stage in polyelectrolyte semiconductor composite films. Degradability of the biopolymers should be further explored to assess the health impact of the possible degraded products.

The non-biodegradable plastic waste depositions on land and seas are one of the conspicuous challenges that we are facing. There are environmental and economic motives to produce 100% bio-based and quickly-enough-biodegradable material for the packaging. There is a need to exploit the natural and renewable resources in a more effective manner. Wood-derived hemicelluloses possess a huge potential in material, pharmaceutical, rheological, and nutritional applications. The challenges arise from the high price of the hemicellulose raw materials due to the absence of large-scale production. However, an advantage of such hemicelluloses is that they do not compete with the existing food resources, as for example starch does. Functionalised GGM has in this study shown to possess a high potential as of barrier coatings in food packaging. Finding several value-added applications will increase the attractiveness of using hemicelluloses in the near future.

8. Acknowledgements

Special thanks go to Professor Stefan Willför for giving me the opportunity to carry out this PhD study, and by guiding me through this rather challenging task with an academic and industrial nature. I appreciate Docent Chunlin Xu due to his skilful consultancy in various aspects of chemistry and material applications and encouragement in working; to my own surprise, I became also appealed to the organic material science via his suggestions with this study. I address the compliments for Jarl (Jalle) Hemming who professionally taught me chemical analysis. Jalle was always ready to help. Docent Andrey Pranovich masters chemistry and the chemistry of natural products. I constantly learnt more by discussing with him about the relevant issues for carrying out this research. Hanna Lindqvist kindly introduced me hemicellulose modification and Professor Emeritus Markku Auer advised me with his vast experience of the research and development in the chemical industry. Leif Österholm was always ready to provide the appropriate facilities for the experimental research. Docent Anna Sundberg warm-hearted revised this thesis. Päivi Pennanen taught me well, how to operate NMR. I am grateful for the support and help for Anders, Affi, Jens, Daniel, Sylwia, Jun, Matti, Risto, Janne, Katja, Annika, Patrik, Rainer, Petri, Robin, Christer, Basti, Lari, Joakim, Outi, Sina, Klaus, Otto, Joakim, Zhiqiang, Wenyang, Bjarne, Markku, Matias and all the who have been working in the Laboratory of Wood and Paper Chemistry and who have helped during the course of this PhD work. The friends are always there: cheers Kristian, Olli, Pasi, Mika, Tao, Peter and Silviu.

I am deeply grateful for the support and help of my wife Ilona who has patiently been there for me and children. It has been a real joy to see my daughters Larissa, Elise and Sonja to grow up. I express thankfulness to my mother Sinikka and father Viktor for providing me the enthusiasm for science. I feel also gratitude to the parents of my wife, my sister Irina and brother Klaus and their families. Irina died in cancer in 1999, yet the wonderful memories of her remain.

This work was carried out in the framework of the Future Biorefinery Project of the Finnish Funding Agency for Technology and Innovation and FIBIC Ltd. I am grateful for the graduate school of Bioregs that provided interesting seminars and financial aid for the networking at the international conferences.

References

Aulin, C., Gällstedt, M., and Lindström, T. (2010). Oxygen and oil barrier properties of microfibrillated cellulose films and coatings. Cellulose *17*, 559–574.

Aulin, C., Karabulut, E., Tran, A., Wågberg, L., and Lindström, T. (2013). Transparent nanocellulosic multilayer thin films on polylactic acid with tunable gas barrier properties. ACS Appl. Mater. Interfaces *5*, 7352–7359.

Auzély-Velty, R. (2011). Self-assembling polysaccharide systems based on cyclodextrin complexation: Synthesis, properties and potential applications in the biomaterials field. Comptes Rendus Chim. *14*, 167–177.

Beesh, M., Majewska, P., and Vandamme, T.F. (2010). Synthesis and characterization of dextran esters as coating or matrix systems for oral delivery of drugs targeted to the colon. Int. J. Drug Deliv. *2*, 22–31.

Begley, T.H., White, K., Honigfort, P., Twaroski, M.L., Neches, R., and Walker, R.A. (2005). Perfluorochemicals: Potential sources of and migration from food packaging. Food Addit. Contam. *22*, 1023–1031.

Belmokaddem, F.-Z., Pinel, C., Huber, P., Petit-Conil, M., and Da Silva Perez, D. (2011). Green synthesis of xylan hemicellulose esters. Carbohydr. Res. *346*, 2896–2904.

Bendoraitiene, J., Kavaliauskaite, R., Klimaviciute, R., and Zemaitaitis, A. (2006). Peculiarities of starch cationization with glycidyltrimethylammonium chloride. Starch - Stärke *58*, 623–631.

Bhaumik, P., Deepa, A.K., Kane, T., and Dhepe, P.L. (2014). Value addition to lignocellulosics and biomass-derived sugars: An insight into solid acid-based catalytic methods. J. Chem. Sci. Bangalore India *126*, 373–385.

Bigand, V., Pinel, C., Da Silva Perez, D., Rataboul, F., Huber, P., and Petit-Conil, M. (2011). Cationisation of galactomannan and xylan hemicelluloses. Carbohydr. Polym. *85*, 138–148.

Böckenhoff, K., and Fischer, W. (2001). Determination of electrokinetic charge with a particle-charge detector, and its relationship to the total charge. Fresenius J. Anal. Chem. *371*, 670–674.

Bollström, R., Saarinen, J.J., Räty, J., and Toivakka, M. (2012). Measuring solvent barrier properties of paper. Meas. Sci. Technol. *23*, 015601/1–015601/8.

Bordenave, N., Grelier, S., and Coma, V. (2010). Hydrophobization and antimicrobial activity of chitosan and paper-based packaging material. Biomacromolecules *11*, 88–96.

Bratskaya, S., Schwarz, S., Laube, J., Liebert, T., Heinze, T., Krentz, O., Lohmann, C., and Kulicke, W.-M. (2005). Effect of polyelectrolyte structural features on flocculation behavior: cationic polysaccharides vs. synthetic polycations. Macromol. Mater. Eng. *290*, 778–785.

Caratzoulas, S., Davis, M.E., Gorte, R.J., Gounder, R., Lobo, R.F., Nikolakis, V., Sandler, S.I., Snyder, M.A., Tsapatsis, M., and Vlachos, D.G. (2014). Challenges of and insights into acid-catalyzed transformations of sugars. J. Phys. Chem. C *118*, 22815–22833.

Chatterjee, C., Pong, F., and Sen, A. (2014). Chemical conversion pathways for carbohydrates. Green Chem. Ahead of Print.

Ciusa, W., and Adamo, G. (1951). Derivatives of starch. IV. Ann. Chim. Rome Italy *41*, 733–738.

Cunha, A.G., and Gandini, A. (2010). Turning polysaccharides into hydrophobic materials: a critical review. Part 2. Hemicelluloses, chitin/chitosan, starch, pectin and alginates. Cellulose *17*, 1045–1065.

Dax, D., Eklund, P., Hemming, J., Sarfraz, J., Backman, P., Xu, C., and Willför, S. (2013a). Amphiphilic spruce galactoglucomannan derivatives based on naturally-occurring fatty acids. BioResources *8*, 3771–3790, 20 pp.

Dax, D., Xu, C., Långvik, O., Hemming, J., Backman, P., and Willför, S. (2013b). Synthesis of SET-LRP-induced galactoglucomannan-diblock copolymers. J. Polym. Sci. Part Polym. Chem. *51*, 5100–5110.

Dax, D., Chavez, M.S., Xu, C., Willför, S., Mendonca, R.T., and Sanchez, J. (2014). Cationic hemicellulose-based hydrogels for arsenic and chromium removal from aqueous solutions. Carbohydr. Polym. *111*, 797–805.

Deuss, P.J., Barta, K., and de Vries, J.G. (2014). Homogeneous catalysis for the conversion of biomass and biomass-derived platform chemicals. Catal. Sci. Technol. *4*, 1174–1196.

Dicke, R. (2004). A straight way to regioselectively functionalized polysaccharide esters. Cellulose *11*, 255–263.

Doliška, A., Willför, S., Strnad, S., Ribitsch, V., Kleinschek, K.S., Eklund, P., and Xu, C. (2012). Antithrombotic properties of sulfated wood-derived galactoglucomannans. Holzforschung *66*.

Donabedian, D.H., and McCarthy, S.P. (1998). Acylation of pullulan by ring-opening of lactones. Macromolecules *31*, 1032–1039.

Duanmu, J., Gamstedt, K., Pranovich, A., and Rosling, A. (2010). Studies on mechanical properties of wood fiber reinforced cross-linked starch composites made from enzymatically degraded allylglycidyl ether-modified starch. Compos. Part Appl. Sci. Manuf. *41A*, 1409–1418.

Durand, A., and Dellacherie, E. (2006). Neutral amphiphilic polysaccharides: chemical structure and emulsifying properties. Colloid Polym. Sci. *284*, 536–545.

Ebringerova, A., Hromadkova, Z., Kacurakova, M., and Antal, M. (1994). Quaternized xylans: synthesis and structural characterization. Carbohydr. Polym. *24*, 301–308.

Ebringerová, A., Hromádková, Z., Hříbalová, V., Xu, C., Holmbom, B., Sundberg, A., and Willför, S. (2008). Norway spruce galactoglucomannans exhibiting immunomodulating and radical-scavenging activities. Int. J. Biol. Macromol. *42*, 1–5.

Edlund, U., and Albertsson, A.-C. (2008). A microspheric system: hemicellulose-based hydrogels. J. Bioact. Compat. Polym. *23*, 171–186.

Ekholm, F.S., Ardá, A., Eklund, P., André, S., Gabius, H.-J., Jiménez-Barbero, J., and Leino, R. (2012). Studies related to norway spruce galactoglucomannans: chemical synthesis, conformation analysis, nmr spectroscopic characterization, and molecular recognition of model compounds. Chem. - Eur. J. *18*, 14392–14405.

Ekouevi, K., and Adepoju, A. (1995). Adjustment, social sectors, and demographic change in Sub-Saharan Africa. J. Int. Dev. *7*, 47–59.

Eronen, P., Österberg, M., Heikkinen, S., Tenkanen, M., and Laine, J. (2011). Interactions of structurally different hemicelluloses with nanofibrillar cellulose. Carbohydr. Polym. *86*, 1281–1290.

Escalante, A., Gonçalves, A., Bodin, A., Stepan, A., Sandström, C., Toriz, G., and Gatenholm, P. (2012). Flexible oxygen barrier films from spruce xylan. Carbohydr. Polym. *87*, 2381–2387.

Farris, S., Mora, L., Capretti, G., and Piergiovanni, L. (2012). Charge density quantification of polyelectrolyte polysaccharides by conductometric titration: an analytical chemistry experiment. J. Chem. Educ. *89*, 121–124.

Fujioka, R., Tanaka, Y., and Yoshimura, T. (2009). Synthesis and properties of superabsorbent hydrogels based on guar gum and succinic anhydride. J. Appl. Polym. Sci. *114*, 612–616.

Gatenholm, P., and Tenkanen, M. (2004). Hemicelluloses: Science and technology (American Chemical Society).

Geng, F., Chang, P.R., Yu, J., and Ma, X. (2010). The fabrication and the properties of pretreated corn starch laurate. Carbohydr. Polym. *80*, 360–365.

Grenman, H., Eränen, K., Krogell, J., Willför, S., Salmi, T., and Murzin, D.Y. (2011). Kinetics of aqueous extraction of hemicelluloses from spruce in an intensified reactor system. Ind. Eng. Chem. Res. *50*, 3818–3828.

Gröndahl, M., Gustafsson, A., and Gatenholm, P. (2006). Gas-phase surface fluorination of arabinoxylan films. Macromolecules *39*, 2718–2721.

Guzman, E., Ortega, F., Baghdadli, N., Cazeneuve, C., Luengo, G.S., and Rubio, R.G. (2011). Adsorption of conditioning polymers on solid substrates with different charge density. ACS Appl. Mater. Interfaces *3*, 3181–3188.

Hannuksela, T., and Hervé du Penhoat, C. (2004). NMR structural determination of dissolved O-acetylated galactoglucomannan isolated from spruce thermomechanical pulp. Carbohydr. Res. *339*, 301–312.

Hansen, N.M.L., and Plackett, D. (2008). Sustainable Films and Coatings from Hemicelluloses: A Review. Biomacromolecules *9*, 1493–1505.

Hansen, N.M.L., Blomfeldt, T.O.J., Hedenqvist, M.S., and Plackett, D.V. (2012). Properties of plasticized composite films prepared from nanofibrillated cellulose and birch wood xylan. Cellul. Dordr. Neth. *19*, 2015–2031.

Hartman, J., Albertsson, A.-C., and Sjöberg, J. (2006). Surface- and bulk-modified galactoglucomannan hemicellulose films and film laminates for versatile oxygen barriers. Biomacromolecules *7*, 1983–1989.

Heinze, T., Haack, V., and Rensing, S. (2004). Starch derivatives of high degree of functionalization. 7. Preparation of cationic 2-hydroxypropyltrimethylammonium chloride starches. Starch/Stärke *56*, 288–296.

Heinze, T., Liebert, T., and Koschella, A. (2006). Esterification of polysaccharids (Springer Berlin Heidelberg).

Henriksson, M., Henriksson, G., Berglund, L.A., and Lindström, T. (2007). An environmentally friendly method for enzyme-assisted preparation of microfibrillated cellulose (MFC) nanofibers. Eur. Polym. J. *43*, 3434–3441.

Henriksson, M., Berglund, L.A., Isaksson, P., Lindström, T., and Nishino, T. (2008). Cellulose nanopaper structures of high toughness. Biomacromolecules *9*, 1579–1585.

Hirrien, M., Desbrieres, J., and Rinaudo, M. (1997). Physical properties of methyl celluloses in relation to the conditions for cellulose modification. Carbohydr. Polym. *31*, 243–252.

Hirvikorpi, T., and Valtion teknillinen tutkimuskeskus (2011). Thin Al_2O_3 barrier coatings grown on bio-based packaging materials by atomic layer deposition. VTT.

Institute of European Bioplastics and Biocomposites (2013). Bioplastics, facts and figures. http://www.google.fi/url?sa=t&rct=j&q=&esrc=s&source=web&cd=1&ved=0CB8QFjAA&url=http%3A%2F%2Fwww.corbion.com%2Fmedia%2F203221%2Feubp_factsfigures_bioplastics_2013.pdf&ei=VTtoVbquDoOLsgGdyIGoCA&usg=AFQjCNEHHs8fofrBuyCKqu18gjR5nKQj1g&bvm=bv.93990622,d.bGg

Isogai, A. (2013). Wood nanocelluloses: fundamentals and applications as new bio-based nanomaterials. J. Wood Sci. *59*, 449–459.

Jana, S.C., and Prieto, A. (2002). Natural fiber composites of high-temperature thermoplastic polymers: Effects of coupling agents. J. Appl. Polym. Sci. *86*, 2168–2173.

Jayasiri, H.B., Purushothaman, C.S., and Vennila, A. (2013). Quantitative analysis of plastic debris on recreational beaches in Mumbai, India. Mar. Pollut. Bull. *77*, 107–112.

Jenkins, P.J., and Donald, A.M. (1998). Gelation of starch: a combined SAXS/WAXS/DSC and SANS study. Carbohydr. Res. *308*, 133–147.

Johansson, C. (2011). Functional barriers against migration for food packaging. In Multifunct. Nanoreinf. Polym. Food Packag., (Woodhead Publishing Ltd.), pp. 316–344.

Jones, J.K.N., Merler, E., and Wise, L.E. (1957). Hemicelluloses present in aspenwood (Populus tremuloides). III. The constitution of pentosan and hexosan fractions. Can. J. Chem. *35*, 634–645.

Kääriäinen, T.O., Maydannik, P., Cameron, D.C., Lahtinen, K., Johansson, P., and Kuusipalo, J. (2011). Atomic layer deposition on polymer based flexible packaging materials: Growth characteristics and diffusion barrier properties. Thin Solid Films *519*, 3146–3154.

Kilpeläinen, P., Kitunen, V., Pranovich, A., Ilvesniemi, H., and Willför, S. (2013). Pressurized hot water flow-through extraction of birch sawdust with acetate pH buffer. BioResources *8*, 5202–5218, 17 pp.

Kilpeläinen, P.O., Hautala, S.S., Byman, O.O., Tanner, L.J., Korpinen, R.I., Lillandt, M.K.-J., Pranovich, A.V., Kitunen, V.H., Willför, S.M., and Ilvesniemi, H.S. (2014). Pressurized hot water flow-through extraction system scale up from the laboratory to the pilot scale. Green Chem. *16*, 3186.

Kim, J.Y., Lee, J.K., Lee, T.S., and Park, W.H. (2003). Synthesis of chitooligosaccharide derivative with quaternary ammonium group and its antimicrobial activity against Streptococcus mutans. Int. J. Biol. Macromol. *32*, 23–27.

Kjellgren, H., Gällstedt, M., Engström, G., and Järnström, L. (2006). Barrier and surface properties of chitosan-coated greaseproof paper. Carbohydr. Polym. *65*, 453–460.

Kochumalayil, J.J., Zhou, Q., Kasai, W., and Berglund, L.A. (2013). Regioselective modification of a xyloglucan hemicellulose for high-performance biopolymer barrier films. Carbohydr. Polym. *93*, 466–472.

Krogell, J., Korotkova, E., Eränen, K., Pranovich, A., Salmi, T., Murzin, D., and Willför, S. (2013). Intensification of hemicellulose hot-water extraction from spruce wood in a batch extractor - Effects of wood particle size. Bioresour. Technol. *143*, 212–220.

Kuusipalo, J., and Lahtinen, K. (2005). Influence of temperature and mixing ratio on water vapor barrier properties of extrusion-coated paper. Int. J. Polym. Anal. Charact. *10*, 71–83.

Kuutti, L., Haavisto, S., Hyvärinen, S., Mikkonen, H., Koski, R., Peltonen, S., Suortti, T., and Kyllönen, H. (2011). Properties and flocculation efficiency of cationized biopolymers and their applicability in papermaking and in conditioning of pulp and paper sludge. BioResources *6*, 2836–2850.

Kwak, S.-Y., Jung, S.G., and Kim, S.H. (2001). Structure-motion-performance relationship of flux-enhanced reverse osmosis (ro) membranes composed of aromatic polyamide thin films. Environ. Sci. Technol. *35*, 4334–4340.

Laine, C., Harlin, A., Hartman, J., Hyvärinen, S., Kammiovirta, K., Krogerus, B., Pajari, H., Rautkoski, H., Setälä, H., Sievänen, J., et al. (2013). Hydroxyalkylated xylans - Their synthesis and application in coatings for packaging and paper. Ind. Crops Prod. *44*, 692–704.

Leppänen, A.-S., Xu, C., Liu, J., Wang, X., Pesonen, M., and Willför, S. (2013). Anionic polysaccharides as templates for the synthesis of conducting polyaniline and as structural matrix for conducting biocomposites. Macromol. Rapid Commun. *34*, 1056–1061.

Leppänen, A.-S., Xu, C., Parikka, K., Eklund, P., Sjöholm, R., Brumer, H., Tenkanen, M., and Willför, S. (2014). Targeted allylation and propargylation of galactose-containing polysaccharides in water. Carbohydr. Polym. *100*, 46–54.

Leslie, T., Xiao, H., and Dong, M. (2005). Tailor-modified starch/cyclodextrin-based polymers for use in tertiary oil recovery. J. Pet. Sci. Eng. *46*, 225–232.

Li, Y., Hu, M., Xiao, H., Du, Y., Decker, E.A., and McClements, D.J. (2010). Controlling the functional performance of emulsion-based delivery systems using multi-component biopolymer coatings. Eur. J. Pharm. Biopharm. *76*, 38–47.

Lindqvist, H., Holmback, J., Rosling, A., Salminen, K., Holmbom, B., Auer, M., and Sundberg, A. (2013). Galactoglucomannan derivatives and their application in papermaking. BioResources *8*, 994–1010, 17 pp.

Liu, J., Willför, S., and Xu, C. (2015). A review of bioactive plant polysaccharides: Biological activities, functionalization, and biomedical applications. Bioact. Carbohydr. Diet. Fibre *5*, 31–61.

Lozhechnikova, A., Dax, D., Vartiainen, J., Willför, S., Xu, C., and Österberg, M. (2014). Modification of nanofibrillated cellulose using amphiphilic block-structured galactoglucomannans. Carbohydr. Polym. *110*, 163–172.

Lundström-Hämälä, L., Johansson, E., and Wågberg, L. (2010). Polyelectrolyte multilayers from cationic and anionic starch: influence of charge density and salt concentration on the properties of the adsorbed layers. Starch - Stärke *62*, 102–114.

Manasrah, M. Al, Kallioinen, M., Ilvesniemi, H., and Mänttäri, M. (2012). Recovery of galactoglucomannan from wood hydrolysate using regenerated cellulose ultrafiltration membranes. Bioresour. Technol. *114*, 375–381.

Martins, J.T., Cerqueira, M.A., Bourbon, A.I., Pinheiro, A.C., Souza, B.W.S., and Vicente, A.A. (2012). Synergistic effects between κ-carrageenan and locust bean gum on physicochemical properties of edible films made thereof. Food Hydrocoll. *29*, 280–289.

Michielsen, S. (1999). Specific refractive index increments of polymers in dilute solu-tions (New York: Wiley).

References

Mielonen, K., Geydt, P., Österberg, M., Johansson, L.-S., and Backfolk, K. (2015). Inkjet ink spreading on polyelectrolyte multilayers deposited on pigment coated paper. J. Colloid Interface Sci. *438*, 179–190.

Mihindukulasuriya, S.D.F., and Lim, L.-T. (2014). Nanotechnology development in food packaging: A review. Trends Food Sci. Technol. *40*, 149–167.

Mikkonen, K.S., Heikkinen, S., Soovre, A., Peura, M., Serimaa, R., Talja, R.A., Helén, H., Hyvönen, L., and Tenkanen, M. (2009). Films from oat spelt arabinoxylan plasticized with glycerol and sorbitol. J. Appl. Polym. Sci. *114*, 457–466.

Mikkonen, K.S., Heikkilä, M.I., Helen, H., Hyvönen, L., and Tenkanen, M. (2010). Spruce galactoglucomannan films show promising barrier properties. Carbohydr. Polym. *79*, 1107–1112.

Mikkonen, K.S., Stevanic, J.S., Joly, C., Dole, P., Pirkkalainen, K., Serimaa, R., Salmen, L., and Tenkanen, M. (2011). Composite films from spruce galactoglucomannans with microfibrillated spruce wood cellulose. Cellul. Dordr. Neth. *18*, 713–726.

Mikkonen, K.S., Schmidt, J., Vesterinen, A.-H., and Tenkanen, M. (2013). Crosslinking with ammonium zirconium carbonate improves the formation and properties of spruce galactoglucomannan films. J. Mater. Sci. *48*, 4205–4213.

Miller, K.S., and Krochta, J.M. (1997). Oxygen and aroma barrier properties of edible films: review. Trends Food Sci. Technol. *8*, 228–237.

Mittal, V. (2011). Bio-nanocomposites: future high-value material. In Nanocomposites with Biodegradable Polymers, Synthesi, Properties and Future Perspectives, (Oxford University Press),.

Moad, G. (2010). Chemical modification of starch by reactive extrusion. Prog. Polym. Sci. *36*, 218–237.

Nyström, J. (2014). Mikroplast det dolda hotet i havet. Forsk. Framsteg 34–39.

Oinonen, P., Areskogh, D., and Henriksson, G. (2013). Enzyme catalyzed cross-linking of spruce galactoglucomannan improves its applicability in barrier films. Carbohydr. Polym. *95*, 690–696.

Pahimanolis, N., Salminen, A., Penttilä, P.A., Korhonen, J.T., Johansson, L.-S., Ruokolainen, J., Serimaa, R., and Seppälä, J. (2013). Nanofibrillated cellulose/carboxymethyl cellulose composite with improved wet strength. Cellulose *20*, 1459–1468.

Peng, F., Peng, P., Xu, F., and Sun, R.-C. (2012). Fractional purification and bioconversion of hemicelluloses. Biotechnol. Adv. *30*, 879–903.

Pigorsch, E. (2009). Spectroscopic characterisation of cationic quaternary ammonium starches. Starch - Stärke *61*, 129–138.

Polari, L., Ojansivu, P., Mäkelä, S., Eckerman, C., Holmbom, B., and Salminen, S. (2012). Galactoglucomannan Extracted from Spruce (*Picea abies*) as a Carbohydrate Source for Probiotic Bacteria. J. Agric. Food Chem. *60*, 11037–11043.

Ramesh, H.P., and Tharanathan, R.N. (2003). Carbohydrates - the renewable raw materials of high biotechnological value. Crit. Rev. Biotechnol. *23*, 149–173.

Ramesh, H., and Tharanatha, R. Carbohydrates - The Renewable Raw Matrieals of High Biotechnolgical Value.

Ren, J., Peng, X., Zhong, L., Feng, P., and Sun, R. (2012). Novel hydrophobic hemicelluloses: Synthesis and characteristic. Carbohydr. Polym. *89*, 152–157.

Ren, J.-L., Liu, C.-F., Sun, R.-C., She, D., and Liu, J.-C. (2007). Preparation and characterization of sugarcane bagasse hemicellulosic derivatives containing quaternary ammonium groups in various media. E-Polym. No pp. given.

Ren, J.L., Peng, F., Sun, R.C., Liu, C.F., Cao, Z.N., Luo, W., and Tang, J.N. (2008). Synthesis of cationic hemicellulosic derivatives with a low degree of substitution in dimethyl sulfoxide media. J. Appl. Polym. Sci. *109*, 2711–2717.

Ren, J.-L., Peng, F., Sun, R.-C., and Kennedy, J.F. (2009). Influence of hemicellulosic derivatives on the sulfate kraft pulp strength. Carbohydr. Polym. *75*, 338–342.

Rissanen, J.V., Grenman, H., Xu, C., Willför, S., Murzin, D.Y., and Salmi, T. (2014). Obtaining Spruce Hemicelluloses of Desired Molar Mass by using Pressurized Hot Water Extraction. ChemSusChem *7*, 2947–2953.

Roos, A.A., Edlund, U., Sjöberg, J., Albertsson, A.-C., and Stålbrand, H. (2008). Protein release from galactoglucomannan hydrogels: influence of substitutions and enzymatic hydrolysis by β-mannanase. Biomacromolecules *9*, 2104–2110.

Sableviciene, D., Klimaviciute, R., Bendoraitiene, J., and Zemaitaitis, A. (2005). Flocculation properties of high-substituted cationic starches. Colloids Surf. Physicochem. Eng. Asp. *259*, 23–30.

Sail, D., and Kováč, P. (2012). Benzoylated ethyl 1-thioglycosides: direct preparation from per-O-benzoylated sugars. Carbohydr. Res. *357*, 47–52.

Salam, A., Venditti, R.A., Pawlak, J.J., and El-Tahlawy, K. (2011). Crosslinked hemicellulose citrate–chitosan aerogel foams. Carbohydr. Polym. *84*, 1221–1229.

Schmidt, V.C.R., Porto, L.M., Laurindo, J.B., and Menegalli, F.C. (2013). Water vapor barrier and mechanical properties of starch films containing stearic acid. Ind. Crops Prod. *41*, 227–234.

Schoeler, B., Delorme, N., Doench, I., Sukhorukov, G.B., Fery, A., and Glinel, K. (2006). Polyelectrolyte films based on polysaccharides of different conformations: effects on multilayer structure and mechanical properties. Biomacromolecules *7*, 2065–2071.

Von Schoultz, S. (2014). Method for extracting biomass. Patent number WO 2014009604 A1

Sehaqui, H., Zhou, Q., Ikkala, O., and Berglund, L.A. (2011). Strong and tough cellulose nanopaper with high specific surface area and porosity. Biomacromolecules *12*, 3638–3644.

Shah, A.A., Hasan, F., Hameed, A., and Ahmed, S. (2008). Biological degradation of plastics: A comprehensive review. Biotechnol. Adv. *26*, 246–265.

Siracusa, V., Rocculi, P., Romani, S., and Rosa, M.D. (2008). Biodegradable polymers for food packaging: a review. Trends Food Sci. Technol. *19*, 634–643.

Song, T., Pranovich, A., Sumerskiy, I., and Holmbom, B. (2008). Extraction of galactoglucomannan from spruce wood with pressurised hot water. Holzforschung *62*.

Spiridon, I., Teacă, C.-A., Bodîrlău, R., and Bercea, M. (2013). Behavior of cellulose reinforced cross-linked starch composite films made with tartaric acid modified starch microparticles. J. Polym. Environ. *21*, 431–440.

Stevanic, J., Bergström, E., Gatenholm, P., Berglund, L., and Salmen, L. (2012). Arabinoxylan/nanofibrilated cellulose composite films. J. Mater. Sci. *47*, 6724–6732.

Stevanic, J.S., Mikkonen, K.S., Xu, C., Tenkanen, M., Berglund, L., and Salmén, L. (2014). Wood cell wall mimicking for composite films of spruce nanofibrillated cellulose with spruce galactoglucomannan and arabinoglucuronoxylan. J. Mater. Sci. *49*, 5043–5055.

Stojanovic, Z., Jeremic, K., and Jovanovic, S. (2002). Synthesis of starch benzoate in aqueous media. Polym. Bull. Berl. Ger. *49*, 265–272.

Suciu, N.A., Tiberto, F., Vasileiadis, S., Lamastra, L., and Trevisan, M. (2013). Recycled paper-paperboard for food contact materials: Contaminants suspected and migration into foods and food simulant. Food Chem. *141*, 4146–4151.

Sun, R.C., Fang, J.M., Tomkinson, J., Geng, Z.C., and Liu, J.C. (2001). Fractional isolation, physico-chemical characterization and homogeneous esterification of hemicelluloses from fast-growing poplar wood. Carbohydr. Polym. *44*, 29–39.

Tan, W.-F., Norde, W., and Koopal, L.K. (2011). Humic substance charge determination by titration with a flexible cationic polyelectrolyte. Geochim. Cosmochim. Acta *75*, 5749–5761.

Thamae, T., and Bailie, C. (2008). Natural fibre composites, turning waste into useful materials (VDM Verlag Dr Muller Aktiengesellschaft & Co. Kg).

Thomas, L.C. (2001). Use of multiple heating rate DSC and modulated temperature DSC to detect and analyze temperature-time-dependent transitions in materials. Am. Lab. Shelton Conn. *33*, 26, 28, 30–31.

Thomsen, M.H., Thygesen, A., and Thomsen, A.B. (2008). Hydrothermal treatment of wheat straw at pilot plant scale using a three-step reactor system aiming at high hemicellulose recovery, high cellulose digestibility and low lignin hydrolysis. Bioresour. Technol. *99*, 4221–4228.

Tian, D., Wu, X., Liu, C., and Xie, H.-Q. (2010). Synthesis and flocculation behavior of cationic konjac glucomannan containing quaternary ammonium substituents. J. Appl. Polym. Sci. *115*, 2368–2374.

Timell, T., and Syracuse, N. (1967). Recent progress in the chemistry of wood hemicelluloses. Wood Sci. Technol. *1*, 45–70.

Trovatti, E., Fernandes, S.C.M., Rubatat, L., Perez, D. da S., Freire, C.S.R., Silvestre, A.J.D., and Neto, C.P. (2012). Pullulan–nanofibrillated cellulose composite films with improved thermal and mechanical properties. Compos. Sci. Technol. *72*, 1556–1561.

van Tuil, R., Fowler, P., Lawther, M., and Weber, C. (2000). Properties of biobased packaging materials in Biobased packaging materials for the food industry; Status and perspectives (KVL, Frederiksberg, Denmark,).

Um, B.-H., and van Walsum, G.P. (2010). Evaluation of enzyme mixtures in releasing fermentable sugars from pre-pulping extracts of mixed northeast hardwoods. Appl. Biochem. Biotechnol. *161*, 432–447.

Vartiainen, J., Vahä-Nissi, M., and Harlin, A. (2014). Biopolymer films and coatings in packaging applications-a review of recent developments. Mater. Sci. Appl. *5*, 708–718.

Vincendon, M. (1998). Xylan derivatives: benzyl ethers, synthesis, and characterization. J. Appl. Polym. Sci. *67*, 455–460.

Voepel, J., Edlund, U., and Albertsson, A.-C. (2009). Alkenyl-functionalized precursors for renewable hydrogels design. J. Polym. Sci. Part Polym. Chem. *47*, 3595–3606.

Wei, Y., Cheng, F., and Zheng, H. (2008). Synthesis and flocculating properties of cationic starch derivatives. Carbohydr. Polym. *74*, 673–679.

Whittaker, P., Clarke, J.J., San, R.H.C., Begley, T.H., and Dunkel, V.C. (2008). Evaluation of the butter flavoring chemical diacetyl and a fluorochemical paper additive for mutagenicity and toxicity using the mammalian cell gene mutation assay in L5178Y mouse lymphoma cells. Food Chem. Toxicol. *46*, 2928–2933.

Willför, S., Rehn, P., Sundberg, A., Sundberg, K., and Holmbom, B. (2003a). Recovery of water solube acetylglucomannans from mechanical pulp of spruce. Tappi J. *2*, 27–32.

Willför, S., Sjöholm, R., Laine, C., Roslund, M., Hemming, J., and Holmbom, B. (2003b). Characterisation of water-soluble galactoglucomannans from Norway spruce wood and thermomechanical pulp. Carbohydr. Polym. *52*, 175–187.

Willför, S., Sundberg, K., Tenkanen, M., and Holmbom, B. (2008). Spruce-derived mannans – A potential raw material for hydrocolloids and novel advanced natural materials. Carbohydr. Polym. *72*, 197–210.

Xu, C., Pranovich, A., Vähäsalo, L., Hemming, J., Holmbom, B., Schols, H.A., and Willför, S. (2008). Kinetics of Acid Hydrolysis of Water-Soluble Spruce O-Acetyl Galactoglucomannans. J. Agric. Food Chem. *56*, 2429–2435.

Xu, C., Willför, S., Holmlund, P., and Holmbom, B. (2009a). Rheological properties of water-soluble spruce O-acetyl galactoglucomannans. Carbohydr. Polym. *75*, 498–504.

Xu, C., Pranovich, A., Hemming, J., Holmbom, B., Albrecht, S., Schols, H.A., and Willför, S. (2009b). Hydrolytic stability of water-soluble spruce O-acetyl galactoglucomannans. Holzforschung *63*.

Xu, C., Leppänen, A.-S., Eklund, P., Holmlund, P., Sjöholm, R., Sundberg, K., and Willför, S. (2010). Acetylation and characterization of spruce (Picea abies) galactoglucomannans. Carbohydr. Res. *345*, 810–816.

Xu, C., Eckerman, C., Smeds, A., Reunanen, M., Eklund, P.C., Sjöholm, R., and Willför, S. (2011). Carboxymethylated spruce galactoglucomannans: preparation, characterization, dispersion stability, water-in-oil emulsion stability, and sorption on cellulose surface. Nord. Pulp Pap. Res. J. *26*, 167–178.

Xu, C., Spadiut, O., Araújo, A.C., Nakhai, A., and Brumer, H. (2012). Chemo-enzymatic Assembly of Clickable Cellulose Surfaces via Multivalent Polysaccharides. ChemSusChem *5*, 661–665.

Yaich, A.I., Edlund, U., and Albertsson, A.-C. (2014). Adapting wood hydrolysate barriers to high humidity conditions. Carbohydr. Polym. *100*, 135–142.

Yu, H., Huang, Y., Ying, H., and Xiao, C. (2007). Preparation and characterization of a quaternary ammonium derivative of konjac glucomannan. Carbohydr. Polym. *69*, 29–40.

Zhou, Q., Greffe, L., Baumann, M.J., Malmström, E., Teeri, T.T., and Brumer, H. (2005). Use of xyloglucan as a molecular anchor for the elaboration of polymers from cellulose surfaces: a general route for the design of biocomposites. Macromolecules *38*, 3547–3549.

References

Österberg, M., Vartiainen, J., Lucenius, J., Hippi, U., Seppälä, J., Serimaa, R., and Laine, J. (2013). A fast method to produce strong NFC films as a platform for barrier and functional materials. ACS Appl. Mater. Interfaces *5*, 4640–4647.

Åbo Akademi

BIOREGS

FIBIC
FINNISH BIOECONOMY CLUSTER

Johan Gadolin
Process Chemistry Centre

9 789521 232862 >

ISBN 978-952-12-3286-2